JOC The Journal of Organic Chemistry

Featured Article

pubs.acs.org/joc

Triazole- and Tetrazole-Bridged Nucleic Acids: Synthesis, Duplex Stability, Nuclease Resistance, and in Vitro and in Vivo Antisense Potency

Yasunori Mitsuoka,[†,‡] Tsuyoshi Yamamoto,[†] Akira Kugimiya,[*,‡] Reiko Waki,[†] Fumito Wada,[†] Saori Tahara,[†] Motoki Sawamura,[†] Mio Noda,[†] Yuko Fujimura,[‡] Yuki Kato,[§] Yoshiyuki Hari,[†,∥] and Satoshi Obika[*,†]

[†]Graduate School of Pharmaceutical Sciences, Osaka University, 1-6 Yamadaoka, Suita Osaka 565-0871, Japan

[‡]Discovery Research Laboratory for Innovative Frontier Medicines, Shionogi & Co., Ltd., 3-1-1 Futaba-cho, Toyonaka, Osaka 561-0825, Japan

[§]Research Laboratory for Development, Shionogi & Co., Ltd., 3-1-1 Futaba-cho, Toyonaka, Osaka 561-0825, Japan

[∥]Faculty of Pharmaceutical Sciences, Tokushima Bunri University, Nishihama, Yamashiro-cho, Tokushima 770-8514, Japan

Supporting Information

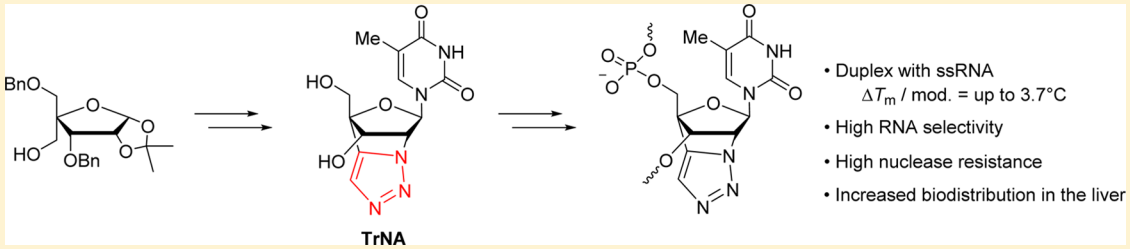

ABSTRACT: Antisense oligonucleotides are attractive therapeutic agents for several types of disease. One of the most promising modifications of antisense oligonucleotides is the introduction of bridged nucleic acids. As we report here, we designed novel bridged nucleic acids, triazole-bridged nucleic acid (TrNA), and tetrazole-bridged nucleic acid (TeNA), whose sugar conformations are restricted to N-type by heteroaromatic ring-bridged structures. We then successfully synthesized TrNA and TeNA and introduced these monomers into oligonucleotides. In UV-melting experiments, TrNA-modified oligonucleotides exhibited increased binding affinity toward complementary RNA and decreased binding affinity toward complementary DNA, although TeNA-modified oligonucleotides were decomposed under the annealing conditions. Enzymatic degradation experiments demonstrated that introduction of TrNA at the 3′-terminus rendered oligonucleotides resistant to nuclease digestion. Furthermore, we tested the silencing potencies of TrNA-modified antisense oligonucleotides using in vitro and in vivo assays. These experiments revealed that TrNA-modified antisense oligonucleotides induced potent downregulation of gene expression in liver. In addition, TrNA-modified antisense oligonucleotides showed a tendency for increased liver biodistribution. Taken together, our findings indicate that TrNA is a good candidate for practical application in antisense methodology.

INTRODUCTION

Antisense technology continues to gain attention as a novel and innovative drug discovery platform with potential applications beyond those of conventional small-molecule- and antibody-based strategies. As seen with Kynamro, the first systemic antisense drug approved by FDA in 2013,[1] specific chemical modifications endow antisense oligonucleotides (ASOs) with increased binding affinity toward complementary RNA in a sequence-specific manner. RNA selectivity and high nuclease resistance are also essential for clinical application of ASOs.[2,3] In this context, multiple kinds of chemical modifications have been developed for use in antisense strategies.[4,5] Restriction of the sugar conformation by a bridged structure between the 2′- and 4′-positions is one important strategy to increase affinity of ASOs toward complementary RNA and improve resistance to nuclease degradation.[6,7] 2′-*O*,4′-*C*-Methylene-bridged nucleic acid (2′,4′-bridged nucleic acid, 2′,4′-BNA, or locked nucleic acid, LNA) exhibits unprecedentedly high binding affinity toward complementary RNA and moderate resistance to enzymatic degradation (Figure 1).[8−12]

Since the discovery of 2′,4′-BNA/LNA, a number of analogues of this class have been designed and synthesized, providing further improvements of properties beyond those of the first generation of 2′,4′-BNA/LNA.[13−22] The previous reports have employed the following structure expansion strategies: the replacement of 2′-oxygen with nitrogen (2′-amino-LNA[13]), sulfur (2′-thio-LNA[14]), carbon (carba-LNA[15]),

Received: October 12, 2016
Published: December 2, 2016

DOI: 10.1021/acs.joc.6b02417
J. Org. Chem. 2017, 82, 12−24

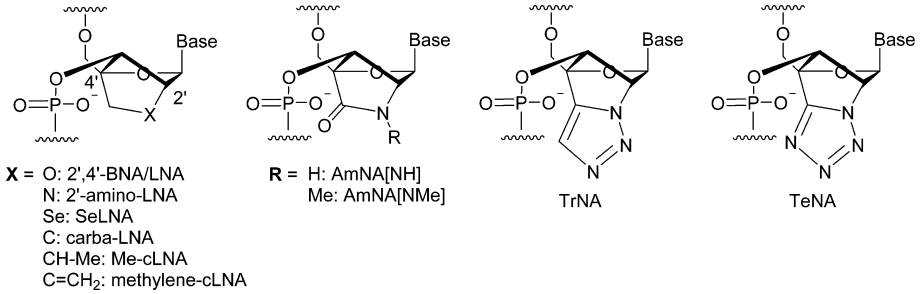

Figure 1. Structures of 2′-substituted 2′,4′-BNA/LNA analogues, AmNA[NR], TrNA, and TeNA.

Scheme 1[a]

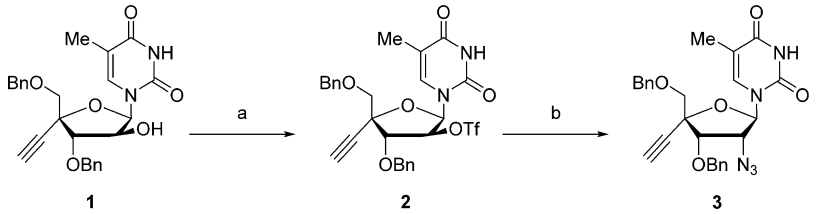

[a]Reagents and conditions: (a) Tf_2O, pyridine, CH_2Cl_2, 0 °C; (b) NaN_3, DMF, 40 °C, 72% over two steps.

and selenium (SeLNA[16]); introduction of substituents at the C6′ site in 2′,4′-BNA/LNA;[17,18] and introduction of substituents at the C6′ and C7′ sites in carba-LNA[15,19−22] (Figure 1). We also recently reported the synthesis and properties of amido-bridged nucleic acids (AmNAs[23]) (Figure 1). Introduction of substituents at the bridge moiety in 2′,4′-BNA/LNA enhanced RNA selectivity and nuclease resistance because of increasing steric hindrance.[15,18−20,23] Although multiple 2′,4′-BNA/LNA analogues have been reported, there have not been any examples of artificial nucleic acids that employ the aromatic ring as a bridge structure. The synthesis of novel bridged nucleic acids containing aromatic rings as the bridged structures, and characterization of oligonucleotides incorporating these modifications, would be of great interest. As we report here, we have designed two novel heteroaromatic ring-bridged nucleic acids, which we have designated triazole-bridged nucleic acid (TrNA) and tetrazole-bridged nucleic acid (TeNA). The triazole and tetrazole are both five-membered heteroaromatic rings having 6π-electron systems, which lead to high electron densities and planar structures. The bridge structures of TrNA and TeNA are relatively large in size, which contributes to acquisition of high RNA selectivity and high nuclease resistance. We also noted that there were no reports describing the synthesis of the structure of 6,7-dihydro-4*H*-4,7-methano[1,2,3]triazolo[5,1-*c*][1,4]oxazine (i.e., a triazole-bridged structure) or 5,6-dihydro-8*H*-5,8-methanotetrazolo-[5,1-*c*][1,4]oxazine (i.e., a tetrazole-bridged structure).

High binding affinity toward complementary RNA and high nuclease resistance are key properties of ASOs. Additionally, the pharmacokinetics of ASOs is another important parameter for the improvement of in vivo activity and safety of ASOs. While we recently reported the successful improvement of liver disposition of ASOs by altering *N*-substituents in AmNAs with maintaining RNase H-recruiting activity,[24] we failed to show an improvement of in vivo knockdown activity of ASOs. In this context, the development of novel bridged nucleic acids is still demanding and challenging. Heteroaromatic structures are often seen in small molecular drugs, suggesting that these domains are potentially biocompatible structures. In general, such moieties are introduced into small drugs not only to increase compound potency but also to alter physicochemical properties to improve pharmacokinetics.[25] Therefore, hetero-aromatic ring-bridged structures are expected to change the physicochemical properties of modified oligonucleotides, possibly leading to enhanced in vivo activity in ASOs. Here, we report the synthesis of TrNA and TeNA and describe the properties of oligonucleotides that incorporate those modifications.

RESULTS

Synthesis of TrNA-T. Two synthetic strategies for constructing 6,7-dihydro-4*H*-4,7-methano[1,2,3]triazolo[5,1-*c*]-[1,4]oxazine (a triazole-bridged structure) were considered. One strategy incorporated an intramolecular Huisgen reaction between an ethynyl group at the 4′-position and an azide group at the 2′-position. The other strategy incorporated an intramolecular S_N2 reaction between the 4′- and 2′-positions. Initially, the intramolecular Huisgen reaction was attempted for the construction of a triazole-bridged structure. As shown in Scheme 1, we performed synthesis of precursor **3**, which bears an ethynyl group at the 4′-position and an azide group at the 2′-position for use in the intramolecular Huisgen reaction. Specifically, precursor **3** was generated by triflation of **1**[26] followed by an S_N2 reaction with NaN_3.

The intramolecular reaction of precursor **3** first was attempted by treatment under high-temperature conditions (Table 1, run 1). However, formation of a triazole-bridged structure was not observed. Instead, several reaction conditions including Cu-catalyzed and Ru-catalyzed Huisgen reactions were attempted for formation of the triazole; again, we did not observe formation of the desired product **4** (Table 1, runs 2−4). These results implied that the construction of a triazole-bridged structure via this synthetic route would be difficult.

As an alternative, we investigated construction of the bridged structure by an S_N2 reaction after introduction of the triazole unit on the 4′-carbon. As shown in Scheme 2, Huisgen reaction of **1** with 2,4-dimethoxybenzyl (DMB) azide[27] gave **5**. Triflation of **5** and subsequent removal of the DMB group

DOI: 10.1021/acs.joc.6b02417
J. Org. Chem. 2017, 82, 12−24

Table 1. Attempted Intramolecular Huisgen Cycloaddition of Compound 3

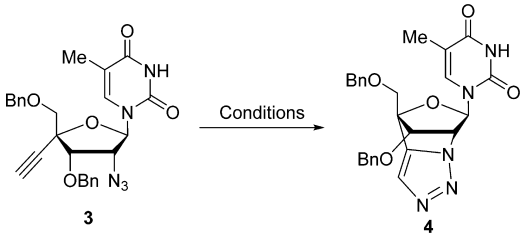

run	conditions	result
1	toluene, 110 °C	no reaction
2	$CuSO_4·5H_2O$ (0.15 equiv), sodium ascorbate (0.5 equiv), THF−H_2O−pyridine, 50 °C	no reaction
3	$CpRuCl(PPh_3)_2$ (0.1 equiv), dioxane, 60 °C	no reaction
4	$CpRuCl(PPh_3)_2$ (0.1 equiv), dioxane, 100 °C	no reaction

with TFA afforded **7**. Subsequent treatment of **7** with K_2CO_3 resulted in intramolecular cyclization to give product **4** (which bears a triazole-bridged structure) in good yield (77% over three steps). Benzyl groups were removed by hydrogenolysis to afford the desired TrNA-T monomer **8**. Finally, dimethoxytritylation of **8** with 4,4′-dimethoxytrityl chloride (DMTrCl) followed by phosphitylation gave the phosphoramidite **10**.

Synthesis of TrNA-^{m}C. For the synthesis of 5-methylcytosine TrNA analogue (TrNA-^{m}C), interconversion of the nucleobase of TrNA-T was performed. As shown in Scheme 3, the secondary hydroxy group of 5′*O*-DMTr-protected compound **9** was protected with a *tert*-butyldimethylsilyl (TBS) group to give **11**. The 4-oxo group of the thymine moiety of **11** was converted into a leaving group by treatment with 2,4,6-triisopropylbenzenesulfonyl chloride (TIPBSCl); subsequent substitution with ammonia afforded a 5-methylcytidine derivative **12**.[28] The exocyclic amino group of the 5-methylcytidine was protected with a benzoyl group by treatment with benzoic anhydride to afford **13**. Compound **13** was treated with triethylamine trihydrofluoride and triethylamine to remove the TBS group. Subsequent phosphitylation of the free secondary hydroxy group yielded the desired 5-methylcytidine phosphoramidite **15**.

Synthesis of TeNA-T. A synthetic strategy similar to that used for TrNA was expected to permit construction of 5,6-dihydro-8*H*-5,8-methanotetrazolo[5,1-*c*][1,4]oxazine (a tetrazole-bridged structure). However, we attempted another synthetic strategy for a tetrazole-bridged structure; we performed a formation of a tetrazole ring from an amide via an activated imidoyl intermediate after construction of an amide-bridged structure because we synthesized the amide-bridged derivative **16**,[23] an intermediate of AmNA. Initially, we attempted the activation of compound **16** using phosphorus pentachloride,[29] but the desired activated imidoyl intermediate was not detected. On the other hand, as shown in Scheme 4, compound **16** was converted into the activated imidoyl intermediate by treatment with triflic anhydride,[30] and a subsequent one-pot reaction with NaN_3 afforded product **17**, which bears a tetrazole-bridged structure. Removal of benzyl and benzyloxymethyl groups by hydrogenolysis followed by

Scheme 2[a]

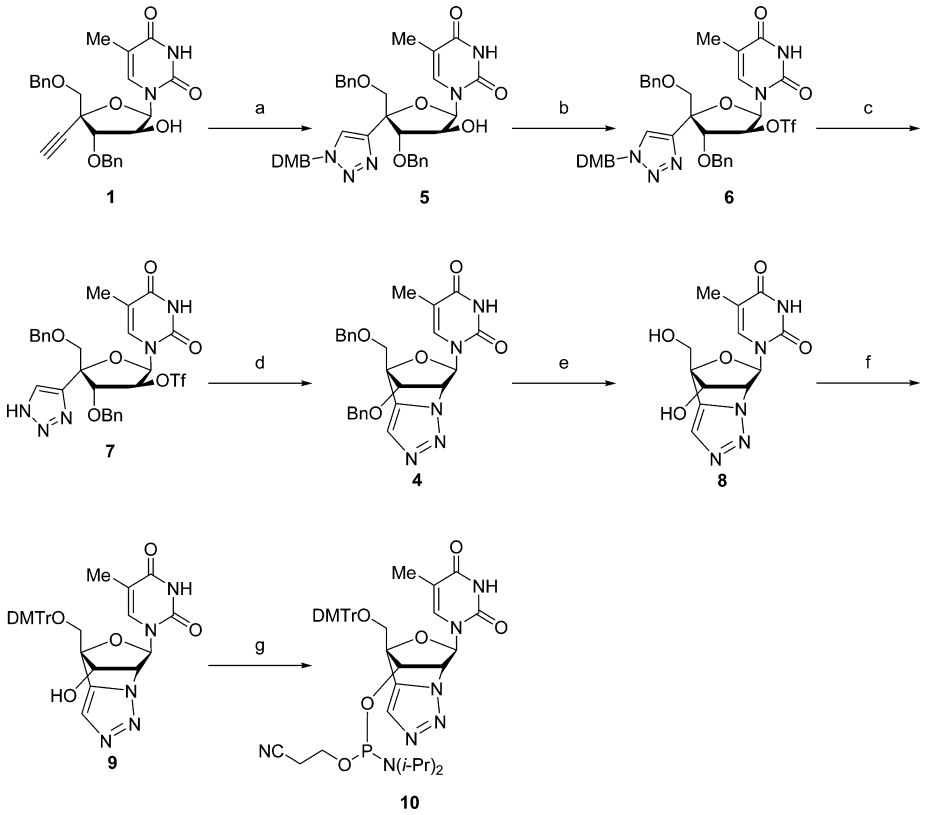

[a]Reagents and conditions: (a) 2,4-dimethoxybenzyl azide, DIPEA, CuI, THF, 70 °C, 99%; (b) Tf_2O, pyridine, CH_2Cl_2, 0 °C; (c) TFA, anisole, 50 °C; (d) K_2CO_3, MeCN, rt, 77% over three steps; (e) $HCOONH_4$, 20% $Pd(OH)_2/C$, EtOH, 85 °C, 24%; (f) DMTrCl, pyridine, rt, 66%; (g) $(i\text{-}Pr_2N)_2POCH_2CH_2CN$, 5-(ethylthio)-1*H*-tetrazole (ETT), MeCN, rt, 81%.

DOI: 10.1021/acs.joc.6b02417
J. Org. Chem. 2017, 82, 12−24

Scheme 3[a]

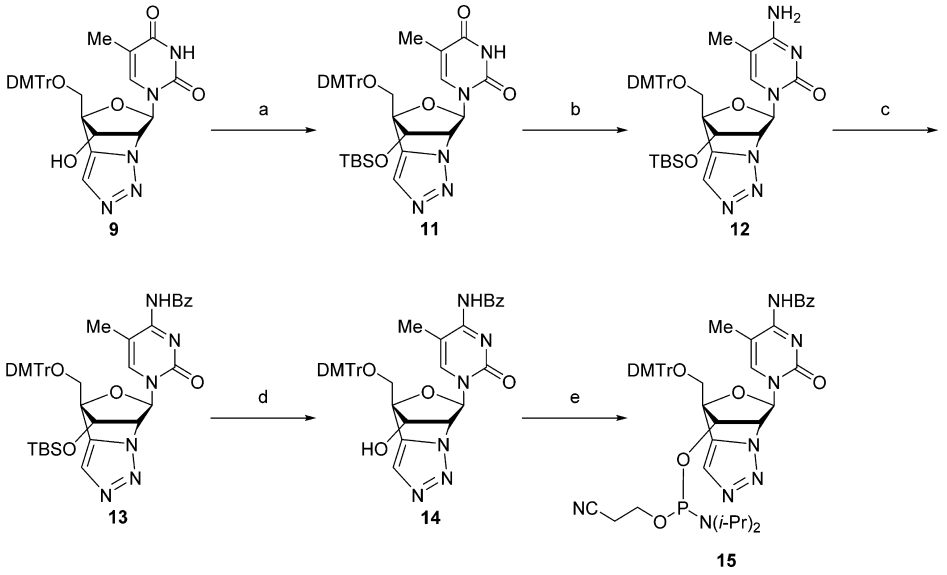

[a]Reagents and conditions: (a) TBSCl, imidazole, DMF, rt, 92%; (b) TIPBSCl, Et_3N, DMAP, MeCN, rt then added 28% NH_3 aq, rt; (c) Bz_2O, DMF, rt, 63% over two steps; (d) $Et_3N{\cdot}3HF$, Et_3N, THF, rt, 92%; (e) $(i\text{-}Pr_2N)_2POCH_2CH_2CN$, ETT, MeCN, rt, 98%.

Scheme 4[a]

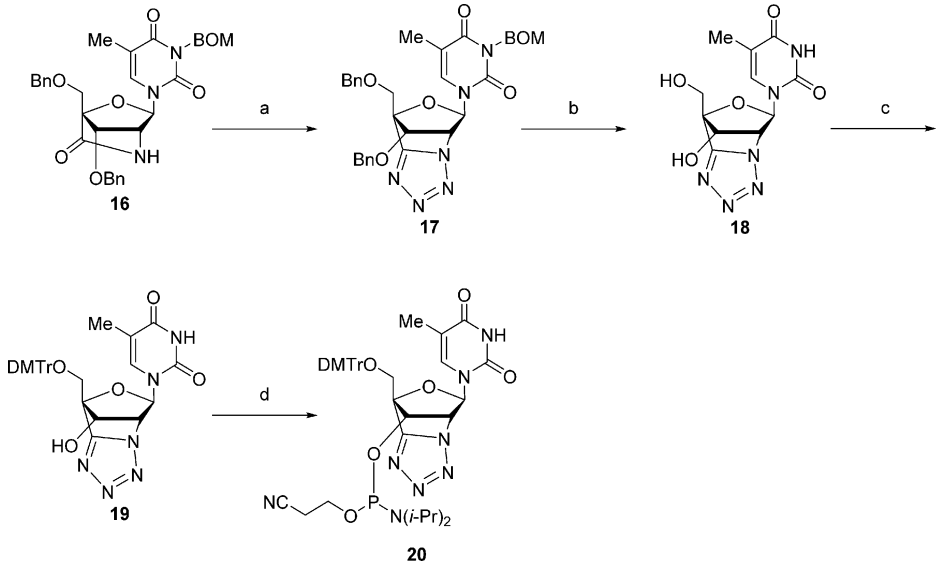

[a]Reagents and conditions: (a) Tf_2O, 2,4,6-trimethylpyridine, MeCN, 0 °C with subsequent addition of NaN_3, rt, 63%; (b) (1) H_2, 20% $Pd(OH)_2/C$, MeOH, rt, (2) 28% NH_3 aq, MeOH−pyridine, rt, quant over two steps; (c) DMTrCl, pyridine, rt, 68%; (d) $(i\text{-}Pr_2N)_2POCH_2CH_2CN$, ETT, MeCN, rt, 89%.

treatment with ammonia to remove the hydroxymethyl groups that remained at the 3N site of thymine gave the desired TeNA-T monomer **18**. Finally, the 5′-position of compound **18** was protected with a DMTr group, and phosphitylation of the 3′-position afforded the phosphoramidite **20**.

Structure of TrNA-T and TeNA-T. The structures of TrNA-T monomer **8** and TeNA-T monomer **18** were confirmed by X-ray crystallography (Figure 2). These crystal structures revealed that the pseudorotation phase angle (P) values were 16.0° (TrNA) and 17.1° (TeNA), indicating an N-type sugar pucker. The maximum torsion angle (ν_{max}) values of the TrNA (56.9°) and TeNA (56.0°) were comparable to those of the corresponding 2′,4′-BNA/LNA (ν_{max} = 56.6°) and AmNA (ν_{max} = 56.9°), indicating that the sugar conformations are very similar (Table 2).

Moreover, the heteroaromatic rings were planar and located perpendicular to the α-face of the furanose ring. The bond lengths in the triazole ring of **8** ranged from 1.33 to 1.37 Å, coinciding well with those of 5,6-dihydro-4*H*-pyrrolo[1,2-*c*][1,2,3]triazole (CCDC 229776) (Figure 3A,B). Similarly, the bond lengths in the tetrazole ring of **18** ranged from 1.31 to 1.39 Å, which agreed well with those of 6,7-dihydro-5*H*-pyrrolo[1,2-*d*]tetrazole (Figure 3C,D).[31] Three methylene carbon atoms of 5,6-dihydro-4*H*-pyrrolo[1,2-*c*][1,2,3]triazole and 6,7-dihydro-5*H*-pyrrolo[1,2-*d*]tetrazole were planar with respect to the planes of the triazole and the tetrazole rings,

DOI: 10.1021/acs.joc.6b02417
J. Org. Chem. 2017, 82, 12−24

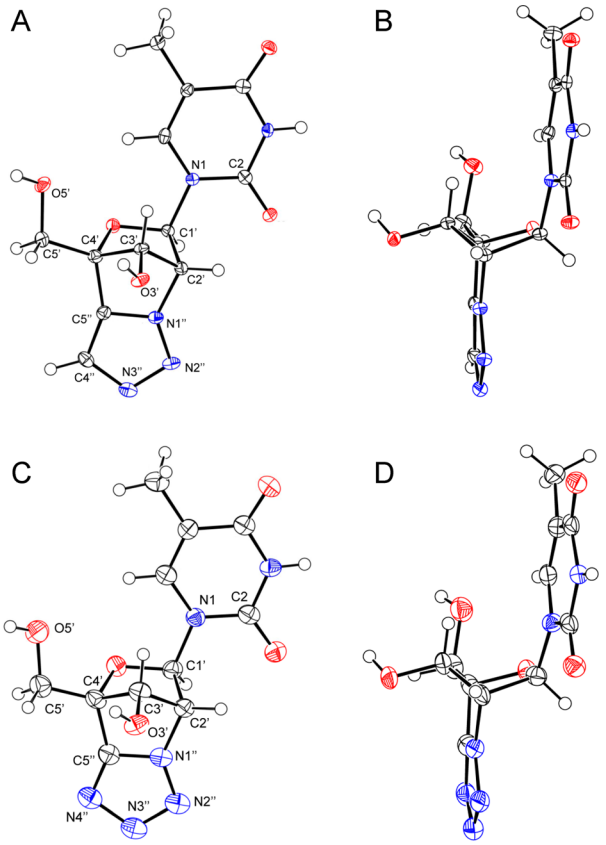

Figure 2. (A, B) X-ray structures of TrNA-T (**8**). (C, D) X-ray structures of TeNA-T (**18**). Displacement ellipsoids are drawn at the 50% probability level.

Table 2. Selected Parameters by X-ray Analysis

	P (deg)	δ (deg)	ν_{max} (deg)
2′,4′-BNA/LNA [8]	17.4	66.2	56.5
AmNA[NMe] [23]	11.6	68.6	56.9
TrNA (**8**)	16.0	68.5	56.9
TeNA (**18**)	17.1	66.8	56.0

respectively. On the other hand, the C3′ carbon atoms of **8** and **18** were out of the planes of the triazole and the tetrazole rings because of the additional bridge moiety. The N1″−C5″−C4′ angle (103.8°) and the C5″−N1″−C2′ angle (111.0°) of **8** and the N1″−C5″−C4′ angle (105.0°) and the C5″−N1″−C2′ angle (111.6°) of **18** were smaller than those of the corresponding 5,6-dihydro-4*H*-pyrrolo[1,2-*c*][1,2,3]triazole and 6,7-dihydro-5*H*-pyrrolo[1,2-*d*]tetrazole (109.6°, 115.6°, 113.5°, and 113.4°, respectively) (Figure 2 and 3).

Oligonucleotide Synthesis. TrNA and TeNA phosphoramidites were incorporated into oligonucleotides using an automated DNA synthesizer with standard phosphoramidite chemistry; 5-ethylthio-1*H*-tetrazole (ETT) was used as an activator. The coupling efficiency of TrNA and TeNA phosphoramidites was decreased under standard conditions, probably due to steric hindrance of the heteroaromatic ring-bridged structures. Prolongation of the coupling time to 16 min from 32 s for TrNA and TeNA phosphoramidites improved the coupling efficiency (over 95% yield). The triazole-bridged structure was stable under conventional conditions (aqueous ammonia at 55 °C and aqueous ammonia and methylamine at room temperature) for cleavage from the resin and removal of protecting groups. On the other hand, the tetrazole-bridged structure did not seem to be as stable as triazole. Notably, some short fragments of oligonucleotide were observed after cleavage from the resin and removal of protecting groups, although the coupling efficiency in the tetrazole-bridged oligonucleotide synthesis still exceeded 95% yield.

Duplex-Forming Abilities of Modified Oligonucleotides. The duplex-forming abilities of the modified oligonucleotides with complementary DNA and RNA were evaluated by UV melting experiments; the resulting values were compared with those for the corresponding natural DNA and 2′,4′-BNA(LNA)-modified oligonucleotides. The melting temperature (T_m) values for duplexes formed by TrNA-modified oligonucleotides **22**−**24** with complementary RNA were higher than that of the duplex formed by the natural DNA **21** and complementary RNA. However, the T_m values for duplexes formed by TrNA-modified oligonucleotides **22**−**24** with complementary RNA were lower than those of 2′,4′-BNA(LNA)-modified oligonucleotides **25**−**27** with complementary RNA (Table 3). ΔT_m modification values ranged from +3.0 to +3.7 °C. In contrast, the TrNA-modified oligonucleotides **22**−**24** destabilized the duplex with complementary DNA, although 2′,4′-BNA(LNA)-modified oligonucleotides **25**−**27** stabilized the duplex with complementary DNA. These results revealed that TrNA-modified oligonucleotides have RNA selective hybridization properties.

In the case of TeNA-modified oligonucleotides, UV melting curves could not be obtained (Figure 4). Since it was expected that the TeNA-modified oligonucleotides decomposed under annealing conditions, we examined the stability of the TeNA-modified oligonucleotides under the same annealing conditions in the absence of a complementary strand. In this experiment, a short fragment that decomposed was observed at the position of TeNA (Supplementary Figure S3).

The decomposition may reflect the release of molecular nitrogen from the bridge moiety at high temperature. Therefore, UV melting experiments for TeNA-modified oligonucleotides were carried out without annealing, although the T_m values obtained without annealing may not be accurate. The T_m values obtained for duplexes formed by TeNA-

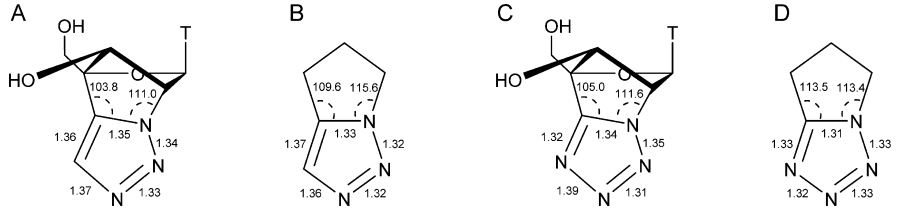

Figure 3. Geometries (bond lengths in Å and angles in deg) of (A) TrNA-T (**8**), (B) 5,6-dihydro-4*H*-pyrrolo[1,2-*c*][1,2,3]triazole, (C) TeNA-T (**18**), and (D) 6,7-dihydro-5*H*-pyrrolo[1,2-*d*]tetrazole.

DOI: 10.1021/acs.joc.6b02417
J. Org. Chem. 2017, 82, 12−24

Table 3. T_m Values (°C) of Oligonucleotides with Complementary DNA and RNA[a]

oligonucleotides	T_m (ΔT_m/mod) DNA complement	T_m (ΔT_m/mod) RNA complement	$T_{m\,(RNA)} - T_{m\,(DNA)}$
5′-GCGTTTTTTGCT-3′ (**21**)	53	49	−4
5′-GCGTTTTTTGCT-3′ (**22**)	52 (−1.0)	52 (+3.0)	0
5′-GCGTTTTTTGCT-3′ (**23**)	51 (−1.0)	56 (+3.5)	+5
5′-GCGTTTTTTGCT-3′ (**24**)	50 (−1.0)	60 (+3.7)	+10
5′-GCGTT*t*TTTGCT-3′ (**25**)	55 (+2.0)	54 (+5.0)	−1
5′-GCGTT*t*T*t*TGCT-3′ (**26**)	57 (+2.0)	59 (+5.0)	+2
5′-GCG*t*T*t*T*t*TGCT-3′ (**27**)	59 (+2.0)	65 (+5.3)	+6

[a]UV melting profiles were measured in 10 mM sodium phosphate buffer (pH 7.2) containing 100 mM NaCl at a scan rate of 0.5 °C/min at 260 nm. The concentration of the oligonucleotide was 4 μM for each strand. T = TrNA-T. *t* = LNA-T. The sequences of target DNA and RNA complements were 5′-d(AGCAAAAAACGC)-3′ and 5′-r(AGCAAAAAACGC)-3′.

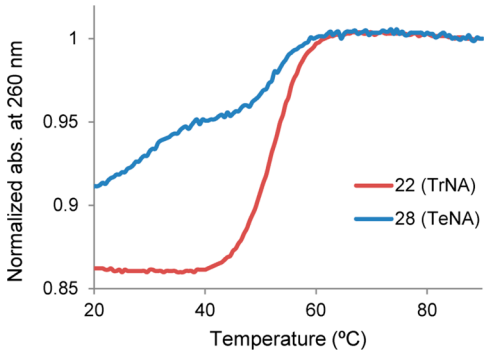

Figure 4. Representative UV melting data of 5′-GCGTTTTTTGCT-3′ with complementary RNA. T = TrNA (red: **22**), TeNA (blue: **28**).

modified oligonucleotides **28**−**30** with complementary strands were slightly lower than those of duplexes formed by TrNA-modified oligonucleotides with complementary strands (Supplementary Table S3).

Enzymatic Stability of Modified Oligonucleotides. The enzymatic stability of TrNA-modified oligonucleotides was evaluated using a 3′-exonuclease; stability was compared with those of the corresponding natural (**31**) and 2′,4′-BNA(LNA)-modified (**32**, **33**) oligonucleotides. Under the conditions used in this experiment, natural oligonucleotide **31** was completely degraded within 5 min. When TrNA or 2′,4′-BNA(LNA) was introduced into the second position from the 3′-terminus, the TrNA-modified oligonucleotide **34** exhibited slightly enhanced stability against the 3′-exonuclease compared to the 2′,4′-BNA(LNA)-modified oligonucleotide **32** (Figure 5A). In contrast, 3′-terminal TrNA-modified oligonucleotide **35** exhibited significantly improved stability against the 3′-exonuclease compared to the corresponding 2′,4′-BNA-(LNA)-modified oligonucleotide **33** (Figure 5B).

Biological Evaluation of Antisense Oligonucleotides. Biological properties of TrNA-modified antisense oligonucleotides were evaluated using two different oligonucleotide sequences (16- and 18-mer) fully modified with the phosphorothioate linkages and targeting mRNA encoding mouse apolipoprotein C-III (*apoC-III* mRNA) (Table 4).[32−34] At the same time, we prepared corresponding 2′,4′-BNA(LNA)-modified ASOs. The 16-mer ASO sequence harbored a 7-mer central DNA gap and corresponds to an oigonucleotide previously described by us in the characterization of the in vivo properties of 2′,4′-BNA(LNA)- and AmNA-modified ASOs.[24] The 18-mer ASO sequence harbored a 9-mer central DNA gap, extending the 7-mer central DNA gap of the 16-mer ASO by the insertion of two DNA nucleotides on the 5′ side of the gap. In a first step, we evaluated the abilities of the modified ASOs to form duplexes with complementary RNA by UV melting experiments. Consistent with the results of the previous experiments, the T_m values for duplexes formed by TrNA-modified ASOs **37** and **40** with complementary RNA were much higher than those of

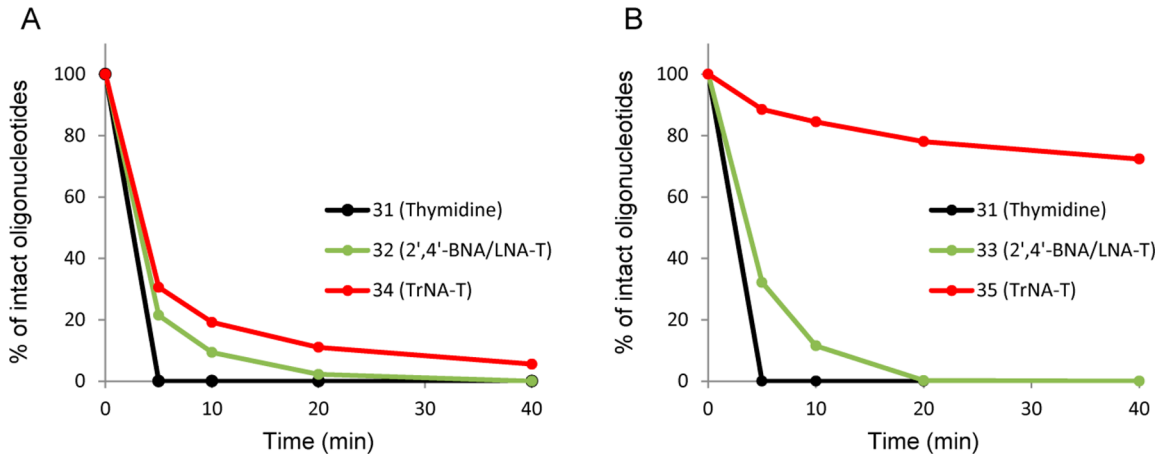

Figure 5. Hydrolysis of oligonucleotides (750 pmol) assessed at 37 °C in buffer (100 μL) containing 50 mM Tris−HCl (pH 8.0), 10 mM $MgCl_2$, and phosphodiesterase I (2.0 mg/mL). Sequences: (A) 5′-d(TTTTTTTTTT)-3′, T = thymidine (black: **31**), 2′,4′-BNA/LNA-T (green: **32**), TrNA-T (red: **34**), (B) 5′-d(TTTTTTTTTT)-3′, T = thymidine (black: **31**), 2′,4′-BNA/LNA-T (green: **33**), TrNA-T (red: **35**).

DOI: 10.1021/acs.joc.6b02417
J. Org. Chem. 2017, 82, 12−24

Table 4. Sequences and T_m Values of Oligonucleotides 36−41[a]

oligonucleotides	T_m (ΔT_m/mod) (°C)
5′-d(TTATCCAGCTTTATTA)-3′ (**36**)	35
5′-d(TTATCCAGCTTTATTA)-3′ (**37**)	56 (+3.5)
5′-d(*tt*A*t*CCAGCTT*t*A*tt*A)-3′ (**38**)	62 (+4.5)
5′-d(TCTTATCCAGCTTTATTA)-3′ (**39**)	42
5′-d(TCTTATCCAGCTTTATTA)-3′(**40**)	58 (+2.7)
5′-d(*tc*T*t*ATCCAGCTT*t*A*tt*A)-3′ (**41**)	63 (+3.5)

[a]UV melting profiles were measured in 10 mM sodium phosphate buffer (pH 7.2) containing 100 mM NaCl at a scan rate of 0.5 °C/min at 260 nm. The concentration of the oligonucleotide was 2 μM for each strand. T = TrNA-T. C = TrNA-^{m}C. *t* = LNA-T. *c* = LNA-^{m}C. All internucleosidic linkages were phosphorothioates. The sequences of target RNA complements were 5′-UAAUAAAGCUGGAUAA-3′ for **36**-**38** and 5′-UAAUAAAGCUGGAUAAGA-3′ for **39**−**41**.

the duplexes formed by the phosphorothioated DNAs **36** and **39** and complementary RNA but lower than those of duplexes formed by 2′,4′-BNA(LNA)-modified ASOs **38** and **41** with complementary RNA (Table 4).

The modified ASOs were next evaluated in cell culture experiments in primary mouse hepatocytes using transfection to provide ASO delivery. The TrNA-modified ASOs **37** and **40** exhibited dose-dependent activity, with both sequences providing activities comparable to those of 2′,4′-BNA(LNA)-modified ASOs **38** and **41** (Figure 6).

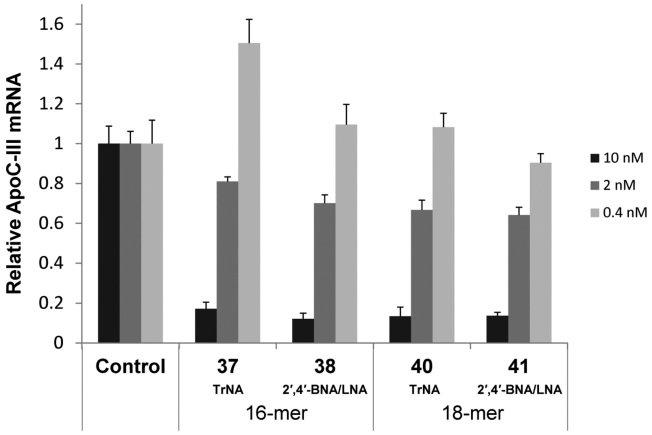

Figure 6. In vitro silencing properties of oligonucleotides. Oligonucleotides were transfected into primary cells (from C57BL/6J mice) at concentrations of 0.4, 2, and 10 nM. After a 24-h incubation, cells were collected and the expression levels of *apoC-III* mRNA (normalized to those of *Gapdh* mRNA) were determined. Data are presented as mean + SD.

In order to assess the mRNA silencing potency of TrNA-modified ASOs **37** and **40** in vivo, we administered ASOs **37**, **38**, **40**, and **41** to C57BL/6J male mice. Mice (n = 4 per dose group) were subjected to tail vein injection with naked ASO at a dosage of 20 mg/kg. At 72 h after the injection, mice were assessed for liver-specific levels of apoC-III mRNA (Figure 7) and ASOs (Figure 8), along with serum toxicological parameters (AST, ALT, BUN, and CRE) (Supplementary Figure S4) and liver histopathology (Supplementary Figure S5). For the 16-mer sequences, the mRNA silencing potency of the TrNA-modified ASO **37** was lower than that of the 2′,4′-BNA(LNA)-modified ASO **38**; tissue levels of the TrNA-

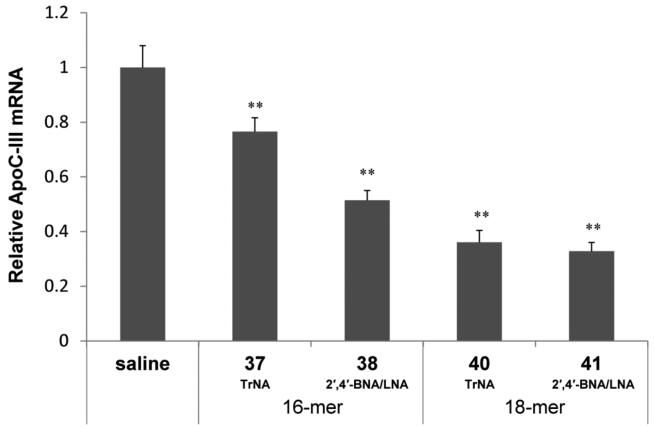

Figure 7. Comparative activity of anti-*apoC-III* antisense oligonucleotides in liver. Liver *apoC-III* mRNA levels (normalized to those of *Gapdh* mRNA) were determined at 72 h after treatment with 20 mg/kg oligonucleotide. Data are presented as mean + SD (n = 4). $^{**}P < 0.01$.

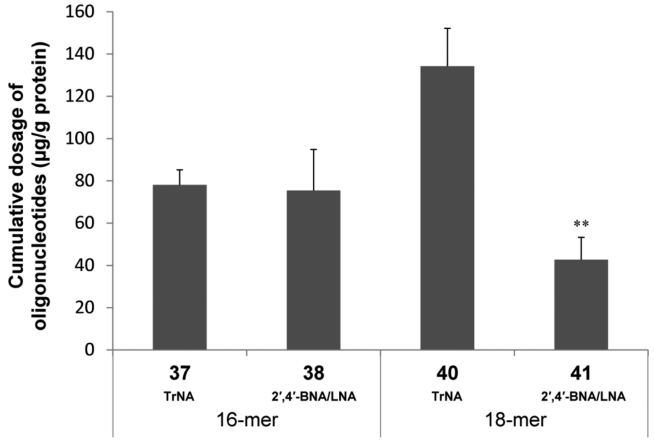

Figure 8. Cumulative dosage of anti-*apoC-III* antisense oligonucleotides in liver. Liver *apoC-III* antisense oligonucleotides levels were determined at 72 h after treatment with 20 mg/kg oligonucleotide. Data are presented as mean + SD (n = 4). $^{**}P < 0.01$ versus TrNA.

modified ASO **37** and 2′,4′-BNA(LNA)-modified ASO **38** did not differ significantly. On the other hand, for the 18-mer sequences, the TrNA-modified ASO **40** and 2′,4′-BNA(LNA)-modified ASO **41** exhibited very similar potencies in silencing, while the tissue level of the TrNA-modified ASO **40** was higher than that of the 2′,4′-BNA(LNA)-modified ASO **41**. There were no significant differences in serum toxicological parameters in the various dosing groups. Histopathologically, no treatment-related changes were observed in any of the ASO-dosed animals.

DISCUSSION

In initial experiments, we were unable to synthesize a triazole-bridged structure by intramolecular Huisgen reaction between the ethynyl group at the 4′-position and the azide group at the 2′-position, despite previous reports of successful use of the intramolecular Huisgen reaction for constructing 5,6-dihydro-4*H*-pyrrolo[1,2-*c*][1,2,3]triazole structures.[35,36] In the transition state for the Huisgen 1,3-dipolar cycloaddition, the ethynyl group and the azide group must be aligned with respect to each other,[37] and the distance between them was calculated to be 2.3 Å.[38] We hypothesize that the construction of a triazole-bridged

DOI: 10.1021/acs.joc.6b02417
J. Org. Chem. 2017, 82, 12−24

structure from **3** imposes steric restrictions on the positions of the ethynyl group and the azide group in a Huisgen reaction, making it difficult for these moieties to be aligned with respect to each other and be within 2.3 Å. On the other hand, the proximity of the nitrogen atom of triazole to the C2′-carbon atom is necessary for the intramolecular S_N2 reaction, and the intramolecular S_N2 reaction gave the desired product **4** bearing a triazole-bridged structure. These results imply that the bridged structure is stable once constructed.

X-ray crystallography revealed that the triazole-bridged structure and the tetrazole-bridged structure were distorted compared to 5,6-dihydro-4*H*-pyrrolo[1,2-*c*][1,2,3]triazole and 6,7-dihydro-5*H*-pyrrolo[1,2-*d*]tetrazole compounds, respectively. The values of the N1″−C5″−C4′ angle and the C5″−N1″−C2′ angle were smaller than those of the corresponding 5,6-dihydro-4*H*-pyrrolo[1,2-*c*][1,2,3]triazole and 6,7-dihydro-5*H*-pyrrolo[1,2-*d*]tetrazole, respectively. In addition, the C3′ carbon atoms were out of the planes of the triazole and the tetrazole rings, although the three methylene carbon atoms in 5,6-dihydro-4*H*-pyrrolo[1,2-*c*][1,2,3]triazole and 6,7-dihydro-5*H*-pyrrolo[1,2-*d*]tetrazole were in the same planes as the triazole and tetrazole rings, respectively. Decomposition of both 1,2,3-triazole and tetrazole include the retro-[3 + 2]-cycloaddition mechanism as an important reaction.[39] 1,2,3-Triazole and tetrazole were found to be decomposed at temperatures of around 599 K (326 °C)[40] and 430 K (157 °C),[41] respectively. Decomposition of the TeNA-T monomer **18** was observed at around 150 °C in measuring melting temperature. The strain of the tetrazole-bridged structure could slightly affect the decomposition of the tetrazole moiety. Although the temperature of the annealing conditions in the present work was lower than the decomposition temperature of tetrazole, the TeNA-modified oligonucleotides decomposed under annealing conditions. We postulate that the buffered solution and the strain of the tetrazole-bridged structure lead to decomposition of tetrazole, resulting in cleavage of TeNA-modified oligonucleotides at the position of the TeNA.

UV melting experiments demonstrated that TrNA-modified oligonucleotides formed stable duplexes with complementary RNA more readily than the natural DNA did. However, the T_m values for duplexes formed by TrNA-modified oligonucleotides with complementary RNA were lower than those of 2′,4′-BNA(LNA)-modified oligonucleotides, even though X-ray crystallography showed that the sugar conformations of TrNA and 2′,4′-BNA/LNA were very similar and that the triazole adopted a planar orientation, as seen for the methylene group of methylene-cLNA[22] and the methyl group of AmNA[NMe].[23] The 2-nitrogen atom of triazole (N2″), which is polar and has a lone pair of electrons, may decrease the T_m values compared to 2′,4′-BNA/LNA. On the other hand, both the methylene group of methylene-cLNA and the methyl group of AmNA[NMe] are nonpolar; this shared property would lead oligonucleotides incorporating these modifications to show similar T_m values compared to 2′,4′-BNA/LNA. In addition, the large triazole-bridged structure may negatively influence the network of hydration around the duplex. On the other hand, the T_m values for duplexes formed by TrNA-modified oligonucleotides with complementary DNA were lower than those of duplexes formed by natural DNA with complementary DNA, while 2′,4′-BNA(LNA)-modified oligonucleotides stabilized the duplex with complementary DNA compared to duplexes formed by natural DNA with complementary DNA. This destabilization of duplexes formed by TrNA-modified oligonucleotides with complementary DNA suggests that the large bridge of TrNA is not as well accommodated in the B-form DNA duplex as the small bridge of 2′,4′-BNA/LNA. Investigation of the entropic and enthalpic components of free energy in the hybridization reaction of TrNA-modified oligonucleotides would clarify the factors affecting the hybridization selectivity of TrNA-modified oligonucleotides.

TrNA exhibited slightly enhanced enzymatic stability against 3′-exonuclease compared to the 2′,4′-BNA/LNA when these modifications were introduced into the second position from the 3′-terminus. In contrast, incorporation of TrNA at the 3′-terminus significantly improved the stability of the resulting oligonucleotide against 3′-exonuclease compared to that of the corresponding 2′,4′-BNA(LNA)-modified oligonucleotide. When introduced at the 3′-terminus, the triazole-bridged structure may cause a steric clash with the nuclease surface and impede access by the metal ion of the nuclease active site.[42] A similar effect on enzymatic stability was observed for oligonucleotides incorporating a guanidine-bridged nucleic acid (GuNA), which has a guanidine moiety in its bridged structure.[43] These results imply that steric properties have a larger influence on stability to 3′-exonuclease than do electronic properties, given that a triazole bridge moiety is neutral, while a guanidine bridge moiety is cationic.

Our in vitro knockdown studies revealed that 18-mer TrNA-modified ASO showed silencing activity comparable to that of 2′,4′-BNA(LNA) congener when delivered to the nucleus using lipofection, while in vitro results with the 16-mer showed slight superiority of 2′,4′-BNA/LNA over TrNA. We propose that these distinctions reflect affinity and steric/electronic differences compared to the respective congeners. In vivo experiments revealed that the hepatic knockdown activity of the respective 16- and 18-mer ASOs reflected their in vitro potencies. However, quantitative analysis of tissue levels of ASOs in liver showed that factors affecting in vivo potency could be different from those affecting in vitro potency. Notably, the knockdown activity of the 18-mer TrNA-modified ASO **40** was similar to that of the conventional 2′,4′-BNA(LNA)-modified ASO **41**, possibly owing to **40**'s more efficient distribution to liver. This difference in liver disposition cannot be attributed simply to a difference in hydrophobicity of the corresponding oligonucleotides. The hydrophobicity of TrNA-T monomer **8** (CLogP: −2.34) is calculated to be lower than that of the 2′,4′-BNA/LNA-T monomer (CLogP: −1.56); HPLC analysis supports this prediction (Supplementary Figure S4). On the other hand, the topological polar surface area (tPSA), regarded as one of the most important indices of the physicochemical properties of molecules,[44] of the TrNA-T monomer **8** (tPSA: 127.06) is estimated to be higher than that of the 2′,4′-BNA/LNA-T monomer (tPSA: 108.33). The tPSA of a modified nucleoside could be an indicator of biodistribution to the liver of oligonucleotides, including those incorporating modified nucleosides, although it is not enough to conclude clear connection between biodistribution and tPSA values. We note, however, that the activity of TrNA-ASOs in our models still varied depending on the length of ASO and the number and position of TrNA. Optimization will be needed to identify the ideal length and residue position for ASOs that incorporate TrNA modifications.

DOI: 10.1021/acs.joc.6b02417
J. Org. Chem. 2017, 82, 12−24

CONCLUSION

In conclusion, we successfully synthesized novel bridged nucleic acids, triazole-bridged nucleic acid (TrNA) and tetrazole-bridged nucleic acid (TeNA), and introduced these monomers into oligonucleotides. We demonstrate that TrNA has interesting features, such as high binding affinity toward complementary RNA, increased RNA selectivity, and elevated nuclease resistance. We additionally showed that TrNA-modified ASOs exhibit increased biodistribution in the liver in an animal model. These results indicate that TrNA is a good candidate for practical application in antisense therapies, especially targeting the liver.

EXPERIMENTAL SECTION

General Experimental Procedure. All reactions were performed under an atmosphere of nitrogen. Unless otherwise mentioned, all chemicals from commercial sources were used without further purification. ^{1}H NMR spectra were recorded at 400 MHz. ^{13}C NMR spectra were recorded at 101 MHz. ^{31}P NMR spectra were recorded at 162 MHz. Chemical shifts are reported in parts per million downfield from tetramethylsilane or deuterated solvent as internal standard for ^{1}H and ^{13}C spectra and 5% H_3PO_4 as external standard for ^{31}P spectra. Mass spectra of all new compounds were measured on fast atom bombardment (FAB) or matrix-assisted laser desorption ionization-time-of-flight (MALDI-TOF) mass spectra. Mass spectra of all new oligonucleotides were measured on electrospray ionization-time-of-flight (ESI-TOF) mass spectra.

*2′-Azido-3′,5′-di-O-benzyl-4′-C-ethynylthymidine (**3**).* Pyridine (0.047 mL, 0.579 mmol) and trifluoromethanesulfonic anhydride (Tf_2O) (0.044 mL, 0.263 mmol) were added to a solution of compound **1**[27] (81 mg, 0.175 mmol) in CH_2Cl_2 (0.8 mL) at 0 °C, and the mixture was stirred at the same temperature for 1 h. After addition of water, the mixture was extracted with EtOAc. The organic extracts were washed with 10% citric acid solution, water, and brine, dried over Na_2SO_4, and concentrated under reduced pressure to give crude compound **2** (113 mg). To a solution of the crude compound **2** (113 mg) in DMF (0.8 mL) was added NaN_3 (46 mg, 0.700 mmol) at room temperature, and the mixture was stirred at 40 °C for 23 h. After addition of water, the mixture was extracted with EtOAc. The organic extracts were washed with saturated aqueous NH_4Cl solution, water, and brine, dried over Na_2SO_4, and concentrated under reduced pressure. The residue was purified by silica gel column chromatography [hexane/EtOAc (85:15 → 60:40, v/v)] to give compound **3** (61 mg, 72% over two steps). White solid. $[\alpha]_D^{23}$ −27.6 (*c* 1.00, $CHCl_3$). IR ν_{max} (KBr): 3276, 3180, 3065, 3034, 2927, 2869, 2112, 1694, 1455, 1362, 1268, 1132, 1088, 1014 cm^{-1}. ^{1}H NMR ($CDCl_3$) δ: 1.60 (3H, s), 2.73 (1H, s), 3.67 (1H, d, *J* = 10.8 Hz), 3.88 (1H, d, *J* = 10.8 Hz), 3.93 (1H, t, *J* = 6.0 Hz), 4.34 (1H, d, *J* = 6.0 Hz), 4.50 (1H, d, *J* = 11.6 Hz), 4.55 (1H, d, *J* = 11.6 Hz), 4.77 (1H, d, *J* = 12.0 Hz), 4.81 (1H, d, *J* = 12.0 Hz), 6.18 (1H, d, *J* = 5.6 Hz), 7.22−7.24 (2H, m), 7.33−7.42 (9H, m), 8.16 (1H, s). ^{13}C NMR ($CDCl_3$) δ_C: 12.1, 63.8, 73.0, 73.7, 73.9, 78.0, 78.4, 78.5, 82.2, 87.1, 111.5, 127.7, 128.2, 128.3, 128.4, 128.6, 128.8, 135.1, 136.7, 136.8, 150.1, 163.4. Mass (FAB): *m*/*z* 510 [M + Na]$^+$. High-resolution MS (FAB): calcd for $C_{26}H_{25}N_5O_5Na$ [M + Na]$^+$ 510.1748, found 510.1758.

*3′,5′-Di-O-Benzyl-4′-C-[1-(2,4-Dimethoxybenzyl)-1H-1,2,3-triazol-4-yl]-5-methyl-arabino-uridine (**5**).* 2,4-Dimethoxybenzyl azide[28] (237 mg, 1.41 mmol), DIPEA (0.16 mL, 0.941 mmol) and CuI (18 mg, 1.41 mmol) were added to a solution of compound **1**[27] (435 mg, 0.941 mmol) in THF (8.7 mL) at room temperature, and the mixture was stirred at 70 °C for 14 h. The mixture was filtered through Celite, and the filtrate was concentrated under reduced pressure. The residue was purified by silica gel column chromatography [hexane/EtOAc (50:50 → 15:85, v/v)] to give compound **5** (613 mg, 99%). White solid. $[\alpha]_D^{26}$ −1.93 (*c* 1.00, $CHCl_3$). IR ν_{max} (KBr): 3187, 3064, 3028, 2938, 1689, 1615, 1509, 1455, 1274, 1210, 1110, 1056 cm^{-1}. ^{1}H NMR ($CDCl_3$) δ: 1.73 (3H, s), 3.73 (3H, s), 3.80 (3H, s), 4.00 (1H, d, *J* = 10.8 Hz), 4.29−4.42 (4H, m), 4.47 (1H, d, *J* = 11.6 Hz), 4.56 (1H, d, *J* = 11.6 Hz), 4.63 (1H, d, *J* = 11.2 Hz), 4.68 (1H, d, *J* = 11.2 Hz), 5.40 (1H, d, *J* = 14.4 Hz), 5.44 (1H, d, *J* = 14.4 Hz), 6.25 (1H, d, *J* = 4.0 Hz), 6.39−6.44 (2H, m), 7.03−7.09 (3H, m), 7.24−7.26 (3H, m), 7.30−7.39 (5H, m), 7.47 (1H, s), 7.57 (1H, s), 8.32 (1H, s). ^{13}C NMR ($CDCl_3$) δ_C: 12.4, 48.9, 55.4, 55.5, 73.1, 73.6, 74.2, 75.0, 85.0, 85.1, 86.0, 98.9, 104.7, 109.5, 115.2, 122.4, 127.5, 127.7, 128.2, 128.3, 128.7, 128.9, 131.2, 136.1, 137.2, 137.3, 145.7, 150.5, 158.4, 161.6, 163.5. Mass (FAB): *m*/*z* 656 [M + H]$^+$. High-resolution MS (FAB): calcd for $C_{35}H_{38}N_5O_8$ [M + H]$^+$ 656.2715, found 656.2720.

*1-[(4R,6R,7R,9R)-9-(Benzyloxy)-4-{(benzyloxy)methyl}-6,7-dihydro-4H-4,7-methano[1,2,3]triazolo[5, 1-c][1,4]oxazin-6-yl]thymine (**4**).* Pyridine (0.239 mL, 2.97 mmol) and Tf_2O (0.228 mL, 1.35 mmol) were added to a solution of compound **5** (589 mg, 0.899 mmol) in CH_2Cl_2 (5.9 mL) at 0 °C, and the mixture was stirred at the same temperature for 40 min. After addition of saturated aqueous $NaHCO_3$ solution, the mixture was extracted with EtOAc. The organic extracts were washed with water and brine, dried over Na_2SO_4, and concentrated under reduced pressure to give crude compound **6** (714 mg). To a solution of the crude compound **6** (714 mg) in TFA (10 mL) was added anisole (0.344 mL, 3.15 mmol) at room temperature, and the mixture was stirred at 50 °C for 2.5 h. After addition of methanol at 0 °C, the mixture was concentrated under reduced pressure. The residue was coevaporated with methanol and toluene to give crude compound **7** (983 mg). To a solution of the crude compound **7** (983 mg) in MeCN (11 mL) was added K_2CO_3 (311 mg, 2.25 mmol) at room temperature, and the mixture was stirred at the same temperature for 5 h. After addition of water, the mixture was extracted with EtOAc. The organic extracts were washed with water and brine, dried over Na_2SO_4, and concentrated under reduced pressure. The residue was purified by silica gel column chromatography [hexane/EtOAc (70:30 → 25:75, v/v)] to give compound **4** (339 mg, 77% over three steps). White solid. $[\alpha]_D^{26}$ +55.3 (*c* 1.00, $CHCl_3$). IR ν_{max} (KBr): 3167, 3063, 3035, 2929, 2871, 2817, 1694, 1456, 1273, 1210, 1161, 1114 cm^{-1}. ^{1}H NMR ($CDCl_3$) δ: 1.65 (3H, d, *J* = 1.2 Hz), 4.14 (1H, d, *J* = 11.2 Hz), 4.37 (1H, d, *J* = 11.2 Hz), 4.54 (1H, d, *J* = 11.6 Hz), 4.58 (1H, d, *J* = 11.6 Hz), 4.65 (1H, s), 4.67 (1H, d, *J* = 11.2 Hz), 4.71 (1H, d, *J* = 11.2 Hz), 5.27 (1H, s), 5.56 (1H, s), 7.10−7.12 (2H, m), 7.28−7.42 (8H, m), 7.56 (1H, d, *J* = 1.2 Hz), 7.63 (1H, s), 8.44 (1H, s). ^{13}C NMR ($CDCl_3$) δ_C: 12.3, 63.8, 65.3, 73.0, 74.1, 84.6, 86.6, 87.0, 111.1, 126.4, 127.8, 128.0, 128.4, 128.7, 128.8, 134.8, 135.6, 136.9, 141.5, 149.5, 163.1. Mass (FAB): *m*/*z* 488 [M + H]$^+$. High-resolution MS (FAB): calcd for $C_{26}H_{26}N_5O_5$ [M + H]$^+$ 488.1928, found 488.1935.

*1-[(4R,6R,7R,9R)-9-Hydroxy-4-(hydroxymethyl)-6,7-dihydro-4H-4,7-methano[1,2,3]triazolo[5,1-c][1,4]oxazin-6-yl]thymine (**8**).* Pd(OH)$_2$−C (20%, 60 mg) and ammonium formate (790 mg, 12.5 mmol) were added to a solution of compound **4** (122 mg, 0.251 mmol) in EtOH (4.9 mL) at room temperature, and the mixture was refluxed for 5.5 h. An additional 20% of Pd(OH)$_2$−C (60 mg) and ammonium formate (790 mg, 12.5 mmol) were added to the mixture at room temperature, and the mixture was refluxed for 1.5 h. The mixture was filtrated through a Celite pad, and Celite was washed with MeOH. The filtrate was concentrated under reduced pressure. The residue was purified by silica gel column chromatography [CH_3Cl/MeOH (100:0 → 85:15, v/v)] to give compound **8** (18 mg, 24%). Colorless block. Mp: 178−180 °C. $[\alpha]_D^{28}$ +29.9 (*c* 0.50, DMSO). IR ν_{max} (KBr): 3434, 3140, 1701, 1658, 1476, 1281 cm^{-1}. ^{1}H NMR (CD_3OD) δ: 1.93 (3H, s), 4.22 (1H, d, *J* = 13.2 Hz), 4.41 (1H, d, *J* = 13.2 Hz), 4.91 (1H, s), 5.22 (1H, s), 5.58 (1H, s), 7.76 (1H, s), 7.87 (1H, s). ^{13}C NMR (CD_3OD) δ_C: 12.7, 57.2, 69.9, 82.2, 86.0, 90.1, 111.4, 127.8, 137.0, 143.9, 152.0, 166.5. Mass (FAB): *m*/*z* 308 [M + H]$^+$. High-resolution MS (FAB): calcd for $C_{12}H_{14}N_5O_5$ [M + H]$^+$ 308.0989, found 308.1001.

*1-[(4R,6R,7R,9R)-4-[{Bis(4-methoxyphenyl)(phenyl)methoxy}methyl]-9-hydroxy-6,7-dihydro-4H-4,7-methano[1,2,3]triazolo[5,1-c][1,4]oxazin-6-yl]thymine (**9**).* 4,4′-Dimethoxytrityl chloride (DMTrCl) (28 mg, 0.083 mmol) was added to a solution of compound **8** (17 mg, 0.055 mmol) in pyridine (0.5 mL) at room temperature. After the mixture was stirred at room temperature for 4 h, additional DMTrCl (28 mg, 0.083 mmol) was added, and the

DOI: 10.1021/acs.joc.6b02417
J. Org. Chem. 2017, 82, 12−24

resulting mixture was stirred at room temperature for 3.5 h. The mixture was diluted with saturated aqueous $NaHCO_3$ solution and extracted with EtOAc. The organic extracts were washed with water and brine, dried over Na_2SO_4, and concentrated under reduced pressure. The residue was purified by silica gel column chromatography [CH_3Cl/MeOH (100:0 → 95:5, v/v)] to give compound **9** (22 mg, 66%). White solid. $[\alpha]_D^{25}$ −12.8 (*c* 1.00, $CHCl_3$). IR ν_{max} (KBr): 3211, 3066, 2933, 2837, 1699, 1607, 1509, 1465, 1254, 1176, 1088, 1034 cm^{-1}. ^1H NMR ($CDCl_3$) δ: 1.67 (3H, s), 3.78 (3H, s), 3.79 (3H, s), 3.90 (1H, d, *J* = 11.6 Hz), 4.02 (1H, d, *J* = 11.6 Hz), 4.33 (1H, brs), 5.15 (1H, d, *J* = 3.6 Hz), 5.23 (1H, s), 5.91 (1H, s), 6.86 (4H, dd, *J* = 8.8, 3.2 Hz), 7.22−7.33 (3H, m), 7.39 (4H, dd, *J* = 8.8, 2.8 Hz), 7.49 (2H, d, *J* = 7.6 Hz), 7.57 (1H, s), 7.74 (1H, s), 9.41 (1H, s). ^{13}C NMR ($CDCl_3$) δ_C: 12.6, 55.3, 57.9, 68.2, 82.4, 84.8, 87.2, 87.7, 111.4, 113.5, 127.2, 127.3, 128.0, 128.2, 130.1, 134.9, 135.0, 135.2, 142.2, 144.2, 150.4, 158.8, 163.9. Mass (FAB): *m*/*z* 610 $[M + H]^+$. High-resolution MS (FAB): calcd for $C_{33}H_{32}N_5O_7$ $[M + H]^+$ 610.2296, found 610.2300.

*(4R,6R,7R,9R)-4-[{Bis(4-methoxyphenyl) (phenyl)methoxy}methyl]-6-(thymin-1-yl)-6,7-dihydro-4H-4,7-methano[1,2,3]triazolo[5,1-c][1,4]oxazin-9-yl(2-cyanoethyl) Diisopropylphosphoramidite (**10**).* 2-Cyanoethyl-*N,N,N′,N′*-tetraisopropylphosphorodiamidite (0.174 mL, 0.549 mmol) and 5-(ethylthio)-1*H*-tetrazole (58 mg, 0.446 mmol) were added to a solution of compound **9** (209 mg, 0.343 mmol) in MeCN (3.0 mL) at room temperature, and the mixture was stirred at the same temperature for 23 h. After addition of saturated aqueous $NaHCO_3$ solution, the mixture was extracted with EtOAc. The organic extracts were washed with water and brine, dried over Na_2SO_4, and concentrated under reduced pressure. The residue was purified by silica gel column chromatography [hexane/EtOAc (50:50 → 25:75, v/v)] to give compound **10** (225 mg, 81%). White solid. ^{31}P NMR ($CDCl_3$) δ_P: 150.4, 150.5. MS (FAB): *m*/*z* 810 $[M + H]^+$. High-resolution MS (FAB): calcd for $C_{42}H_{49}N_7O_8P$ $[M + H]^+$ 810.3375, found 810.3379.

*1-[(4R,6R,7R,9R)-4-[{Bis(4-methoxyphenyl)(phenyl)methoxy}methyl]-9-{(tert-butyldimethylsilyl)oxy}-6,7-dihydro-4H-4,7-methano[1,2,3]triazolo[5,1-c][1,4]oxazin-6-yl]thymine (**11**).* Imidazole (562 mg, 8.26 mmol) and *tert*-butylchlorodimethylsilane (TBSCl) (830 mg, 5.51 mmol) were added to a solution of compound **9** (839 mg, 1.38 mmol) in DMF (6.0 mL) at room temperature, and the mixture was stirred at the same temperature for 18 h. The mixture was diluted with water, and the mixture was extracted with EtOAc. The organic extracts were washed with water and brine, dried over Na_2SO_4, and concentrated under reduced pressure. The residue was purified by silica gel column chromatography [hexane/EtOAc (75:25 → 40:60, v/v)] to give compound **11** (918 mg, 92%). White solid. $[\alpha]_D^{25}$ +7.38 (*c* 1.00, $CHCl_3$). IR ν_{max} (KBr): 3188, 3065, 2955, 2930, 2858, 1697, 1608, 1509, 1464, 1254, 1176, 1082, 1037 cm^{-1}. ^1H NMR ($CDCl_3$) δ: −0.03 (3H, s), 0.02 (3H, s), 0.61 (9H, s), 1.68 (3H, s), 3.65 (1H, d, *J* = 11.2 Hz), 3.80 (6H, s), 4.05 (1H, d, *J* = 11.2 Hz), 5.06 (1H, s), 5.29 (1H, s), 5.57 (1H, s), 6.86 (4H, dd, *J* = 8.8, 4.4 Hz), 7.27−7.37 (7H, m), 7.46 (2H, d, *J* = 7.6 Hz), 7.55 (1H, s), 7.84 (1H, s), 8.25 (1H, s). ^{13}C NMR ($CDCl_3$) δ_C: −5.0, −4.7, 12.7, 17.6, 25.2, 55.3, 57.6, 67.8, 82.4, 85.1, 87.1, 87.9, 111.5, 113.5, 113.5, 126.8, 127.4, 128.0, 128.2, 130.0, 130.1, 134.8, 134.9, 134.9, 141.6, 144.0, 149.6, 159.0, 163.2. Mass (FAB): *m*/*z* 724 $[M + H]^+$. High-resolution MS (FAB): calcd for $C_{39}H_{46}N_5O_7Si$ $[M + H]^+$ 724.3161, found 724.3168.

*N-[1-[(4R,6R,7R,9R)-4-[{Bis(4-methoxyphenyl)(phenyl)methoxy}methyl]-9-{(tert-butyldimethylsilyl)oxy}-6,7-dihydro-4H-4,7-methano[1,2,3]triazolo[5,1-c][1,4]oxazin-6-yl]-5-methylcytidin-4-yl]benzamide (**13**).* Et_3N (0.680 mL, 4.91 mmol), DMAP (30 mg, 0.245 mmol), and 2,4,6-triisopropylbenzenesulfonyl chloride (TIPBSCl) (557 mg, 1.84 mmol) were added to a solution of compound **11** (888 mg, 1.23 mmol) in MeCN (8.9 mL) at room temperature. After the mixture was stirred at room temperature for 18 h, 28% aqueous ammonia solution (8.9 mL) was added at room temperature, and the resulting mixture was stirred at the same temperature for 2 h. MeCN was removed under reduced pressure. The residue was diluted with water, and the mixture was extracted with EtOAc. The organic extracts were washed with water and brine, dried over Na_2SO_4, and concentrated under reduced pressure to give crude compound **12** (1.47 g). To a solution of the crude compound **12** (1.47 g) in DMF (4.5 mL) was added benzoic anhydride (Bz_2O) (361 mg, 1.59 mmol) at room temperature, and the mixture was stirred at the same temperature for 15 h. After addition of saturated aqueous $NaHCO_3$ solution, the mixture was extracted with EtOAc. The organic extracts were washed with water and brine, dried over Na_2SO_4, and concentrated under reduced pressure. The residue was purified by silica gel column chromatography [hexane/EtOAc (80:20 → 60:40, v/v)] to give compound **13** (643 mg, 63% over two steps). White solid. $[\alpha]_D^{25}$ +20.4 (*c* 1.00, $CHCl_3$). IR ν_{max} (KBr): 3065, 2954, 2931, 2857, 1706, 1646, 1572, 1509, 1355, 1309, 1251, 1174, 1081, 1038 cm^{-1}. ^1H NMR ($CDCl_3$) δ: −0.04 (3H, s), 0.02 (3H, s), 0.60 (9H, s), 1.87 (3H, s), 3.66 (1H, d, *J* = 11.2 Hz), 3.81 (6H, s), 4.08 (1H, d, *J* = 11.2 Hz), 5.08 (1H, s), 5.35 (1H, s), 5.63 (1H, s), 6.88 (4H, dd, *J* = 8.8, 5.6 Hz), 7.29−7.40 (7H, m), 7.44−7.49 (4H, m), 7.54−7.57 (2H, m), 8.00 (1H, s), 8.33 (2H, d, *J* = 7.6 Hz), 13.44 (1H, s). ^{13}C NMR ($CDCl_3$) δ_C: −5.0, −4.7, 13.8, 17.6, 25.2, 55.3, 57.6, 67.7, 82.4, 85.3, 87.1, 88.0, 112.7, 113.5, 113.5, 126.8, 127.4, 128.0, 128.2, 128.2, 130.0, 130.1, 132.8, 134.9, 135.0, 135.7, 136.9, 141.6, 144.1, 147.6, 159.0, 159.3, 179.9. Mass (FAB): *m*/*z* 827 $[M + H]^+$. High-resolution MS (FAB): calcd for $C_{46}H_{51}N_6O_7Si$ $[M + H]^+$ 827.3583, found 827.3592.

*N-[1-[(4R,6R,7R,9R)-4-[{Bis(4-methoxyphenyl)(phenyl)methoxy}methyl]-9-hydroxy-6,7-dihydro-4H-4,7-methano[1,2,3]triazolo[5,1-c][1,4]oxazin-6-yl]-5-methylcytidin-4-yl]benzamide (**14**).* Et_3N (0.304 mL, 2.19 mmol) and triethylamine trihydrofluoride (0.714 mL, 4.39 mmol) were added to a solution of compound **13** (605 mg, 0.731 mmol) in THF (6.0 mL) at room temperature, and the mixture was stirred at the same temperature for 1.0 h. After addition of saturated aqueous $NaHCO_3$ solution, the mixture was extracted with EtOAc. The organic extracts were washed with water and brine, dried over Na_2SO_4, and concentrated under reduced pressure. The residue was purified by silica gel column chromatography [CH_3Cl/MeOH (100:0 → 95:5, v/v)] to give compound **14** (482 mg, 92%). White solid. $[\alpha]_D^{25}$ −6.51 (*c* 0.50, $CHCl_3$). IR ν_{max} (KBr): 3071, 2957, 2837, 2790, 1710, 1644, 1600, 1560, 1509, 1359, 1308, 1251, 1175, 1040 cm^{-1}. ^1H NMR ($CDCl_3$) δ: 1.90 (3H, s), 3.35 (1H, brs), 3.81 (3H, s), 3.81 (3H, s), 3.90 (1H, d, *J* = 11.6 Hz), 4.10 (1H, d, *J* = 11.6 Hz), 5.08 (1H, s), 5.25 (1H, s), 5.71 (1H, s), 6.89 (4H, dd, *J* = 8.8, 4.8 Hz), 7.28−7.55 (12H, m), 7.59 (1H, s), 7.89 (1H, s), 8.32 (2H, d, *J* = 5.2 Hz), 13.30 (1H, s). ^{13}C NMR ($CDCl_3$) δ_C: 13.8, 55.3, 55.3, 57.8, 67.9, 81.5, 82.1, 85.0, 87.3, 87.8, 113.2, 113.6, 127.1, 127.2, 127.3, 127.8, 127.9, 128.0, 128.3, 129.2, 130.1, 130.1, 132.9, 135.0, 135.8, 136.8, 139.5, 141.8, 144.3, 147.4, 158.7, 158.9, 158.9, 179.9. Mass (FAB): *m*/*z* 713 $[M + H]^+$. High-resolution MS (FAB): calcd for $C_{40}H_{37}N_6O_7$ $[M + H]^+$ 713.2718, found 713.2730.

*(4R,6R,7R,9R)-6-(4-Benzamido-5-methylcytidin-1-yl)-4-[{bis(4-methoxyphenyl)(phenyl)methoxy}methyl]-6,7-dihydro-4H-4,7-methano[1,2,3]triazolo[5,1-c][1,4]oxazin-9-yl(2-cyanoethyl)-diisopropylphosphoramidite (**15**).* 2-Cyanoethyl-*N,N,N′,N′*-tetraisopropylphosphorodiamidite (0.397 mL, 1.25 mmol) and 5-(ethylthio)-1*H*-tetrazole (122 mg, 0.938 mmol) were added to a solution of compound **14** (446 mg, 0.625 mmol) in MeCN/THF (1:1, v/v, 6.8 mL) at room temperature, and the mixture was stirred at the same temperature for 5.0 h. After addition of saturated aqueous $NaHCO_3$ solution, the mixture was extracted with EtOAc. The organic extracts were washed with water and brine, dried over Na_2SO_4, and concentrated under reduced pressure. The residue was purified by silica gel column chromatography [hexane/EtOAc (65:35 → 45:55, v/v)] to give compound **15** (561 mg, 98%). White solid. ^{31}P NMR ($CDCl_3$) δ_P: 150.8. MS (FAB): *m*/*z* 913 $[M + H]^+$. High-resolution MS (FAB): calcd for $C_{49}H_{54}N_8O_8P$ $[M + H]^+$ 913.3797, found 913.3799.

*1-[(5R,6R,8R,9R)-9-(Benzyloxy)-8-{(benzyloxy)methyl}-5,6-dihydro-8H-5,8-methanotetrazolo[5,1-c][1,4]oxazin-6-yl]-3-{(benzyloxy)methyl}thymine (**17**).* 2,4,6-Trimethylpyridine (0.187 mL, 1.42 mmol) and Tf_2O (0.159 mL, 0.944 mmol) were added to a solution of compound **16**[23] (276 mg, 0.472 mmol) in MeCN (2.7 mL) at 0 °C. After the mixture was stirred at 0 °C for 1.5 h, NaN_3 (123 mg, 1.89 mmol) was added at 0 °C, and the resulting mixture was stirred at room temperature for 1.5 h. After addition of water, the

DOI: 10.1021/acs.joc.6b02417
J. Org. Chem. 2017, 82, 12−24

mixture was extracted with EtOAc. The organic extracts were washed with 2 M aqueous HCl solution, water, and brine, dried over Na_2SO_4, and concentrated under reduced pressure. The residue was purified by silica gel column chromatography [hexane/EtOAc (90:10 → 60:40, v/v)] to give compound **17** (182 mg, 63%). White solid. $[\alpha]_D^{25}$ +50.8 (*c* 1.00, $CHCl_3$). IR ν_{max} (KBr): 3030, 2889, 1711, 1666, 1454, 1283, 1160, 1079 cm^{-1}. ^1H NMR ($CDCl_3$) δ: 1.65 (3H, s), 4.26 (1H, d, *J* = 11.6 Hz), 4.55−4.57 (3H, m), 4.67 (1H, d, *J* = 11.2 Hz), 4.72−4.74 (4H, m), 5.24 (1H, s), 5.45 (1H, d, *J* = 9.6 Hz), 5.48 (1H, d, *J* = 9.6 Hz), 5.52 (1H, s), 7.06−7.08 (2H, m), 7.26−7.39 (13H, m), 7.52 (1H, s). ^{13}C NMR ($CDCl_3$) δ_C: 13.0, 62.6, 65.6, 70.5, 72.5, 73.4, 74.3, 84.5, 85.1, 87.6, 111.0, 127.7, 127.9, 128.0, 128.4, 128.6, 128.8, 128.8, 128.9, 133.0, 135.1, 136.7, 137.8, 150.4, 161.7, 162.8. High-resolution MS (MALDI): calcd for $C_{33}H_{33}N_6O_6$ $[M + H]^+$ 609.2456, found 609.2453.

*1-[(5R,6R,8R,9R)-9-Hydroxy-8-(hydroxymethyl)-5,6-dihydro-8H-5,8-methanotetrazolo[5,1-c][1,4]oxazin-6-yl]thymine (**18**).* Pd-$(OH)_2$-C (20%, 90 mg) was added to a suspension of compound **17** (180 mg, 0.296 mmol) in MeOH (7.5 mL) at room temperature, and the mixture was stirred under an H_2 atmosphere for 18 h. After addition of pyridine, the mixture was filtrated through a Celite pad, and Celite was washed with MeOH/pyridine (1:1, v/v). The filtrate was concentrated under reduced pressure. To a solution of the residue in MeOH/pyridine (1:1, v/v, 5.0 mL) was added 28% aqueous ammonia solution (2.0 mL) at room temperature, and the mixture was stirred at the same temperature for 30 min. The mixture was concentrated under reduced pressure to give compound **18** (98 mg, quant). Colorless platelet. Mp: 150 °C dec. $[\alpha]_D^{28}$ +61.8 (*c* 0.50, DMSO). IR ν_{max} (KBr): 3194, 1669, 1566, 1456, 1276 cm^{-1}. ^1H NMR (DMSO-d_6) δ: 1.86 (3H, d, *J* = 1.2 Hz), 4.17 (1H, dd, *J* = 13.2, 6.0 Hz), 4.42 (1H, dd, *J* = 13.2, 6.0 Hz), 4.96 (1H, d, *J* = 4.0 Hz), 5.34 (1H, s), 5.82 (1H, s), 5.91 (1H, t, *J* = 6.0 Hz), 6.75 (1H, d, *J* = 4.0 Hz), 7.80 (1H, d, *J* = 1.2 Hz), 11.58 (1H, s). ^{13}C NMR (DMSO-d_6) δ_C: 12.4, 54.2, 67.9, 81.5, 83.6, 86.5, 109.2, 134.9, 150.0, 162.4, 163.9. High-resolution MS (MALDI): calcd for $C_{11}H_{12}N_6O_5Na$ $[M + Na]^+$ 331.0761, found 331.0755.

*1-[(5R,6R,8R,9R)-8-[{Bis(4-methoxyphenyl)(phenyl)methoxy}methyl]-9-hydroxy-5,6-dihydro-8H-5,8-methanotetrazolo[5,1-c][1,4]oxazin-6-yl]thymine (**19**).* DMTrCl (134 mg, 0.395 mmol) was added to a solution of compound **18** (72 mg, 0.232 mmol) in pyridine (1.0 mL) at room temperature, and the mixture was stirred at the same temperature for 20 h. The solvent was removed under reduced pressure. The residue was diluted with saturated aqueous $NaHCO_3$ solution, and the mixture was extracted with EtOAc. The organic extracts were washed with water and brine, dried over Na_2SO_4, and concentrated under reduced pressure. The residue was purified by silica gel column chromatography [hexane/EtOAc (55:45 → 30:70, v/v)] to give compound **19** (96 mg, 68%). White solid. $[\alpha]_D^{26}$ −8.69 (*c* 1.00, $CHCl_3$). IR ν_{max} (KBr): 3225, 3065, 2956, 2837, 1696, 1607, 1509, 1464, 1254, 1177, 1035 cm^{-1}. ^1H NMR ($CDCl_3$) δ: 1.58 (3H, s), 3.75 (3H, s), 3.76 (3H, s), 4.02 (1H, d, *J* = 12.0 Hz), 4.12 (1H, brs), 4.31 (1H, d, *J* = 12.0 Hz), 5.26 (1H, s), 5.31 (1H, s), 5.85 (1H, s), 6.84 (4H, dd, *J* = 8.4, 3.6 Hz), 7.20−7.31 (3H, m), 7.36 (4H, dd, *J* = 8.4, 4.8 Hz), 7.46 (2H, d, *J* = 7.6 Hz), 7.79 (1H, s), 9.48 (1H, brs). ^{13}C NMR ($CDCl_3$) δ_C: 12.5, 55.3, 55.3, 56.4, 68.0, 82.8, 84.5, 86.3, 87.5, 111.9, 113.6, 127.3, 127.4, 128.0, 128.2, 128.3, 130.1, 134.8, 134.9, 144.1, 150.3, 158.9, 159.0, 162.2, 164.1. High-resolution MS (MALDI): calcd for $C_{32}H_{29}N_6O_7$ $[M - H]^-$ 609.2103, found 609.2100.

*(5R,6R,8R,9R)-8-[{Bis(4-methoxyphenyl)(phenyl)methoxy}methyl]-6-(thymin-1-yl)-5,6-dihydro-8H-5,8-methanotetrazolo[5,1-c][1,4]oxazin-9-yl(2-cyanoethyl)diisopropylphosphoramidite (**20**).* 2-Cyanoethyl-*N*,*N*,*N*′,*N*′-tetraisopropylphosphorodiamidite (0.149 mL, 0.496 mmol) and 5-(ethylthio)-1*H*-tetrazole (50 mg, 0.381 mmol) were added to a solution of compound **19** (179 mg, 0.293 mmol) in MeCN (2.7 mL) at room temperature, and the mixture was stirred at the same temperature for 15 h. After addition of saturated aqueous $NaHCO_3$ solution, the mixture was extracted with EtOAc. The organic extracts were washed with water and brine, dried over Na_2SO_4, and concentrated under reduced pressure. The residue was purified by silica gel column chromatography [hexane/EtOAc (50:50 → 25:75, v/v)] to give compound **20** (211 mg, 89%). White solid. ^{31}P NMR ($CDCl_3$) δ_P: 150.9, 151.5. High-resolution MS (MALDI): calcd for $C_{41}H_{46}N_8O_8P$ $[M - H]^-$: 809.3182, found 809.3171.

Synthesis, Purification, and Characterization of Oligonucleotides. Syntheses of oligonucleotides were performed on a 0.2 μmol scale (**22**−**24**, **28**−**30**, **34**, **35**) and 3 × 3 μmol scale (**37** and **40**) on an automated DNA synthesizer using the standard phosphoramidite protocol with 0.25 M 5-(ethylthio)-1*H*-tetrazole in acetonitrile as the activator and 0.05 M ((dimethylaminomethylidene)amino)-3*H*-1,2,4-dithiazaoline-3-thione (DDTT) in 3-methylpyridine/acetonitrile (1:1, v/v) for thiolation. The standard synthesis cycle was used for assembly of the reagents and synthesis of the oligonucleotides, except that the coupling time was extended to 16 min for TrNA and TeNA monomers. Oligonucleotide synthesis was performed in DMTr-On mode. Cleavage from the CPG support and removal of the protecting groups were accomplished by using a mixture of 28% aqueous ammonia solution and 40% aqueous methylamine solution (1:1, v/v) at room temperature for 2 h, 28% aqueous ammonia solution at 55 °C for 12−17 h, or 0.1 M NaOH in MeOH/H_2O (4:1, v/v) at room temperature for 15−19 h. In the syntheses of oligonucleotides **22**−**24**, **28**−**30**, **34**, and **35**, the obtained crude oligonucleotides were initially purified using Sep-Pak Plus C18 cartridges, with the 5′-DMT group being removed during purification using 0.5% (v/v) aqueous trifluoroacetic acid (TFA). The separated oligonucleotides were further purified by reversed-phase HPLC [Waters XBridge Shield RP18 Column 5.0 μm, 10 mm × 50 mm (buffer A, 0.1 M TEAA; buffer B, 0.1 M TEAA/MeCN.1:1) or YMC Hydrosphere C18 Column 5.0 μm, 10 mm × 150 mm (buffer A, 0.01 M TEAA; buffer B, 0.01 M TEAA/MeCN.1:1)]. In the syntheses of oligonucleotides **37** and **40**, the obtained crude oligonucleotides were purified by ion-exchange chromatography [GE Healthcare Bioscience, Source 30Q (buffer A, 20 mM Tris·HCl; buffer B, 2.0 M NaBr in A)], with the 5′-DMT group being removed during purification using 3% (v/v) aqueous dichloroacetic acid. Pure fractions were desalted by ultrafiltration. The composition of the oligonucleotides was confirmed by ESI-TOF-MS analysis. HPLC charts and ESI-TOF-MS data of new oligonucleotides are described in the Supporting Information.

UV Melting Experiments (T_m Measurements). UV melting experiments were carried out on UV spectrometers equipped with T_m analysis accessories. The UV melting profiles were recorded in 10 mM sodium phosphate buffer (pH 7.2) containing 100 mM NaCl at a scan rate of 0.5 °C/min with detection at 260 nm. The final concentration of each oligonucleotide was 4 μM (**21**−**30**) or 2 μM (**36**−**41**). The T_m was calculated as the temperature of the half-dissociation of the formed duplexes. The two-point average method was used to obtain the T_m values, and the final values were determined by averaging three independent measurements, which were accurate to within 1 °C.

Degradation of Oligonucleotides by Phosphodiesterase I. Enzymatic degradation experiments were carried out under the following conditions: 2.0 μg/mL phosphodiesterase I, 10 mM $MgCl_2$, 50 mM Tris−HCl buffer (pH 8.0), and 7.5 μM each oligonucleotide, at 37 °C. A portion of each reaction mixture was removed at timed intervals and heated to 90 °C for 5 min to deactivate the enzyme. Aliquots of the timed samples were analyzed by reversed-phase HPLC to evaluate the amount of intact oligonucleotide remaining. The percentage of intact oligonucleotide in each sample was calculated and plotted against the digestion time to obtain a degradation curve.

In Vitro Transfection Study. Hepatocytes were isolated from 7-week-old C57BL/6J male mice using two-step collagenase perfusion in situ as described previously.[45] Briefly, murine liver was perfused with perfusion buffer I via the hepatic portal vein for 5 min at 5 mL/min, followed by perfusion with perfusion buffer II [perfusion buffer I supplemented with 0.1% collagenase (no. C5138, Sigma-Aldrich Japan, Tokyo, Japan) and 0.002% trypsin inhibitor (no. T9128, Sigma-Aldrich Japan, Tokyo, Japan)] for an additional 10 min at 15 mL/min. Hepatocytes isolated from the harvested liver were plated on type-I collagen-coated 96-well plates (no. 4860-010, IWAKI, Tokyo, Japan) at 3 × 10^4 cells/well in William's E medium (10% FBS, 1% penicillin/

DOI: 10.1021/acs.joc.6b02417
J. Org. Chem. 2017, 82, 12−24

streptomycin, 1% GlutaMax (no. 35050061, ThermoFisher Scientific). After 24 h, cells were transfected using Lipofectamine 2000 (no. 11668027, ThermoFisher Scientific) with oligonucleotides at concentrations of 0.4, 2, and 10 nM. After 24 h, total RNA was extracted using a SuperPrep Cell Lysis & RT Kit for qPCR (no. SCQ-101, Toyobo Life Science, Osaka, Japan) according to the manufacturer's instructions. Real-time PCR was performed with TaqMan Fast Advanced Master Mix (no. 4444556, ThermoFisher Scientific) and analyzed with a StepOnePlus system (ThermoFisher Scientific). TaqMan probes were as follows: Mm00445670_m1_FAM (for *Apoc3*) and Mm99999915_g1 _VIC (for *Gapdh*).

Mouse Study. All animal procedures were approved by the Animal Care Ethics Committee of Osaka University. Mice were purchased from CLEA Japan as C57BL/6J males and acclimated for at least 1 week prior to the study start. Studies were initiated when animals were 8 weeks of age. Mice (n = 4/arm) were maintained on a 12-h light/12-h dark cycle and provided ad libitum with food (using standard chow CE-2, CLEA, Japan) and water. Each mouse was administered with a single intravenous dose of saline-formulated ASOs. At 72 h after injection, animals were bled via tail veins, anesthetized with isoflurane (Forane; Abbott, Japan). The whole-blood specimens were collected into BD Microtainer tubes with serum separator additive (no. 365967, BD) and then allowed to clot and centrifuged according to the manufacturer's instructions; the resulting sera were transferred to fresh tubes and stored pending subsequent analysis. Livers were harvested at necropsy and stored in RNA*later* (Life Technologies, no. AM7021) in accordance with the manufacturer's instructions, fixed in 10% neutral buffered formalin (WAKO, no. 062-01661), or snap frozen and stored at −80 °C pending subsequent analysis.

RNA Quantification. Total RNA was isolated from an aliquot (20 mg) of each liver tissue stored in RNA*later* using QuickGene RNA tissue kit SII (RT-S2, Wako, Japan) and QuickGene-810 instrument (KURABO, Japan) according to the manufacturer's procedure. cDNA was synthesized using a high capacity cDNA reverse transcription kit (no. 4368813, ThermoFisher Scientific), and quantitative PCR was performed using TaqMan Fast Universal PCR Master Mix (no. 4352042, ThermoFisher Scientific) and analyzed with a StepOnePlus system (ThermoFisher Scientific). Expression levels of hepatic *Apoc3* mRNA were normalized against those of the *Gapdh* mRNA. TaqMan probes used in quantitative PCR were Mm00445670_m1 for murine *Apoc3* and Mm99999915_g1_VIC for murine *Gapdh*, respectively.

ELISA Method for in Vivo ASO Quantification. Hepatic quantification of ASOs was performed using a previously described ELISA-based method.[46] Specifically, the templates used here were two 25-mer DNAs (5′-gaa tag cga taa taa agc tgg ata a −3′ and 5′-gaa tag cga taa taa agc tgg ata aga-3′) that are complementary to ASOs **36-41**; both templates included a 3′ biotin label. The ligation probe DNA was a 9-mer DNA (5′-tcg cta ttc-3′) with a 5′ phosphate and 3′ digoxigenin.

Serum Chemistry. Serum from blood collected from the inferior vena cava upon sacrifice was subjected to serum chemistry. Serum levels of aspartate aminotransferase (AST), alanine aminotransferase (ALT), blood urea nitrogen (BUN), and creatinine (CRE) were measured using Activity Assay kits (nos. 464-43101, 4460-43201, 279-36201, and 410-39891, Wako, Japan).

Histopathology. The livers of the mice were fixed in 10% neutral buffered formalin (no. 062-01661, Wako), processed, and embedded in paraffin. Paraffin-embedded tissues were sectioned, stained with hematoxylin and eosin (HE), and examined microscopically.

Statistical Analysis. Mouse studies were performed with four mice per treatment group. All data are expressed as mean + SD. Values of $P < 0.01$ were considered to be statistically significant. Two groups were compared using a two-sided Student's t test; more than two groups were compared using Dunnett's test.

X-ray Crystallographic Data. Crystallographic data (excluding structure factors) of **8** and **18** have been deposited at the Cambridge Crystallographic Data Centre. CCDC 1437121 contains the supplementary crystallographic data of **8**, and CCDC 1436990 contains the supplementary crystallographic data of **18**. These data can be obtained free of charge from the Cambridge Crystallographic Data Centre via http://www.ccdc.cam.ac.uk/data_request/cif.

■ ASSOCIATED CONTENT

Supporting Information

The Supporting Information is available free of charge on the ACS Publications website at DOI: 10.1021/acs.joc.6b02417.

X-ray crystallographic data, representative UV melting data, ^{1}H and ^{13}C spectra of **3**−**5**, **8**, **9**, **11**, **13**, **14**, **17**−**19**, ^{31}P spectra of **10**, **15**, and **20**, and HPLC charts and ESI-TOF-MS spectra of new oligonucleotides (PDF)

X-ray crystallographic data of TrNA-T (**8**) and TeNA-T (**18**) (CIF)

■ AUTHOR INFORMATION

Corresponding Authors

*Tel: +81 6 6331 5451. Fax: +81 6 6332 6385. E-mail: akira.kugimiya@shionogi.co.jp.

*Tel: +81 6 6879 8200. Fax: +81 6 6879 8204. E-mail: obika@phs.osaka-u.ac.jp.

ORCID

Satoshi Obika: 0000-0002-6842-6812

Notes

The authors declare no competing financial interest.

■ REFERENCES

(1) Lee, R. G.; Crosby, J.; Baker, B. F.; Graham, M. J.; Crooke, R. M. *J. Cardiovasc. Transl. Res.* **2013**, *6*, 969−980.

(2) Stein, C. A.; Krieg, A. M. *Applied Antisense Oligonucleotide Technology*; Wiley-Liss: New York, 1998.

(3) Schlingensiepen, R.; Brysch, W.; Schlingensiepen, K. H. *Antisense-from Technology to Therapy*; Black Sciences Ltd.: Berlin, 1997.

(4) Yamamoto, T.; Nakatani, M.; Narukawa, K.; Obika, S. *Future Med. Chem.* **2011**, *3*, 339−365.

(5) Sharma, V. K.; Sharma, R. K.; Singh, S. K. *MedChemComm* **2014**, *5*, 1454−1471.

(6) Imanishi, T.; Obika, S. *Chem. Commun.* **2002**, 1653−1659.

(7) Obika, S.; Rahman, S. M. A.; Fujisaka, A.; Kawada, Y.; Baba, T.; Imanishi, T. *Heterocycles* **2010**, *81*, 1347−1392.

(8) Obika, S.; Nanbu, D.; Hari, Y.; Morio, K.; In, Y.; Ishida, T.; Imanishi, T. *Tetrahedron Lett.* **1997**, *38*, 8735−8738.

(9) Obika, S.; Nanbu, D.; Hari, Y.; Andoh, J.; Morio, K.; Doi, T.; Imanishi, T. *Tetrahedron Lett.* **1998**, *39*, 5401−5404.

(10) Singh, S. K.; Nielsen, P.; Koshkin, A. A.; Wengel, J. *Chem. Commun.* **1998**, 455−456.

(11) Koshkin, A. A.; Singh, S. K.; Nielsen, P.; Rajwanshi, V. K.; Kumar, R.; Meldgaard, M.; Olsen, C. E.; Wengel, J. *Tetrahedron* **1998**, *54*, 3607−3630.

(12) Vester, B.; Wengel, J. *Biochemistry* **2004**, *43*, 13233−13241.

(13) Singh, S. K.; Kumar, R.; Wengel, J. *J. Org. Chem.* **1998**, *63*, 10035−10039.

(14) Kumar, R.; Singh, S. K.; Koshkin, A. A.; Rajwanshi, V. K.; Meldgaard, M.; Wengel, J. *Bioorg. Med. Chem. Lett.* **1998**, *8*, 2219−2222.

(15) Xu, J.; Liu, Y.; Dupouy, C.; Chattopadhyaya, J. *J. Org. Chem.* **2009**, *74*, 6534−6554.

(16) Morihiro, K.; Kodama, T.; Kentefu; Moai, Y.; Veedu, R. N.; Obika, S. *Angew. Chem., Int. Ed.* **2013**, *52*, 5074−5078.

(17) Seth, P. P.; Siwkowski, A.; Allerson, C. R.; Vasquez, G.; Lee, S.; Prakash, T. P.; Wancewicz, E. V.; Witchell, D.; Swayze, E. E. *J. Med. Chem.* **2009**, *52*, 10−13.

(18) Seth, P. P.; Vasquez, G.; Allerson, C. A.; Berdeja, A.; Gaus, H.; Kinberger, G. A.; Prakash, T. P.; Migawa, M. T.; Bhat, B.; Swayze, E. E. *J. Org. Chem.* **2010**, *75*, 1569−1581.

DOI: 10.1021/acs.joc.6b02417
J. Org. Chem. 2017, 82, 12−24

(19) Srivastava, P.; Barman, J.; Pathmasiri, W.; Plashkevych, O.; Wenska, M.; Chattopadhyaya, J. *J. Am. Chem. Soc.* **2007**, *129*, 8362−8379.
(20) Zhou, C.; Liu, Y.; Andaloussi, M.; Badgujar, N.; Plashkevych, O.; Chattopadhyaya, J. *J. Org. Chem.* **2009**, *74*, 118−134.
(21) Seth, P. P.; Allerson, C. R.; Berdeja, A.; Siwkowski, A.; Pallan, P. S.; Gaus, H.; Prakash, T. P.; Watt, A. T.; Egli, M.; Swayze, E. E. *J. Am. Chem. Soc.* **2010**, *132*, 14942−14950.
(22) Seth, P. P.; Pallan, P. S.; Swayze, E. E.; Egli, M. *ChemBioChem* **2013**, *14*, 58−62.
(23) Yahara, A.; Shrestha, A. R.; Yamamoto, T.; Hari, Y.; Osawa, T.; Yamaguchi, M.; Nishida, M.; Kodama, T.; Obika, S. *ChemBioChem* **2012**, *13*, 2513−2516.
(24) Yamamoto, T.; Yahara, A.; Waki, R.; Yasuhara, H.; Wada, F.; Harada-Shiba, M.; Obika, S. *Org. Biomol. Chem.* **2015**, *13*, 3757−3765.
(25) Dalvie, D.; Kang, P.; Loi, C. -M.; Goulet, L.; Nair, S. In *Metabolism, Pharmacokinetics and Toxicity of Functional Groups: Impact of Chemical Building Blocks on ADMET*; Smith, D. A., Ed.; Royal Society of Chemistry: Cambridge, 2010; pp 328−369.
(26) Ohrui, H.; Kohgo, S.; Kitano, K.; Sakata, S.; Kodama, E.; Yoshimura, K.; Matsuoka, M.; Shigeta, S.; Mitsuya, H. *J. Med. Chem.* **2000**, *43*, 4516−4525.
(27) van der Knaap, M.; Lageveen, L. T.; Busscher, H. J.; Mars-Groenendijk, R.; Noort, D.; Otero, J. M.; Llamas-Saiz, A. L.; van Raaij, M. J.; van der Marel, G. A.; Overkleeft, H. S.; Overhand, M. *ChemMedChem* **2011**, *6*, 840−847.
(28) Höbartner, C.; Micura, R. *J. Am. Chem. Soc.* **2004**, *126*, 1141−1149.
(29) Kennedy, L. J. *Tetrahedron Lett.* **2010**, *51*, 2010−2013.
(30) Cai, Y.; Ling, C.-C.; Bundle, D. R. *J. Org. Chem.* **2009**, *74*, 580−589.
(31) Ward, D. L.; Wei, K.-T.; Smetana, A. J.; Popov, A. I. *Acta Crystallogr., Sect. B: Struct. Crystallogr. Cryst. Chem.* **1979**, *35*, 1413−1419.
(32) Lee, S.-J.; Campos, H.; Moye, L. A.; Sacks, F. M. *Arterioscler., Thromb., Vasc. Biol.* **2003**, *23*, 853−858.
(33) Yamamoto, T.; Obika, S.; Nakatani, M.; Yasuhara, H.; Wada, F.; Shibata, E.; Shibata, M.-A.; Harada-Shiba, M. *Eur. J. Pharmacol.* **2014**, *723*, 353−359.
(34) Crooke, R. M.; Graham, M. J.; Lemonidis, K. M.; Dobie, K. W. US Patent No. 7598227, 2009.
(35) Guerin, D. J.; Miller, S. J. *J. Am. Chem. Soc.* **2002**, *124*, 2134−2136.
(36) Brawn, R. A.; Welzel, M.; Lowe, J. T.; Panek, J. S. *Org. Lett.* **2010**, *12*, 336−339.
(37) Huisgen, R. *Angew. Chem., Int. Ed. Engl.* **1963**, *2*, 633−696.
(38) Ess, D. H.; Jones, G. O.; Houk, K. N. *Org. Lett.* **2008**, *10*, 1633−1636.
(39) da Silva, G.; Bozzelli, J. W. *J. Org. Chem.* **2008**, *73*, 1343−1353.
(40) Malow, M.; Wehrstedt, K. D.; Neuenfeld, S. *Tetrahedron Lett.* **2007**, *48*, 1233−1235.
(41) Lesnikovich, A. I.; Ivashkevich, O. A.; Lyutsko, V. A.; Printsev, G. V.; Kovalenko, K. K.; Gaponik, P. N.; Levchik, S. V. *Thermochim. Acta* **1989**, *145*, 195−202.
(42) Pallan, P. S.; Allerson, C. R.; Berdeja, A.; Seth, P. P.; Swayze, E. E.; Prakash, T. P.; Egli, M. *Chem. Commun.* **2012**, *48*, 8195−8197.
(43) Shrestha, A. R.; Kotobuki, Y.; Hari, Y.; Obika, S. *Chem. Commun.* **2014**, *50*, 575−577.
(44) Ertl, P. In *Molecular Drug Properties: Measurement and Prediction*; Mannhold, R., Ed.; Wiley-VCH: Weinheim, 2007; pp 111−126.
(45) Shen, L.; Hillebrand, A.; Wang, D. Q. -H.; Liu, M. *J. Visualized Exp.* **2012**, *64*, e3917.
(46) Yamamoto, T.; Harada-Shiba, M.; Nakatani, M.; Wada, S.; Yasuhara, H.; Narukawa, K.; Sasaki, K.; Shibata, M. A.; Torigoe, H.; Yamaoka, T.; Imanishi, T.; Obika, S. *Mol. Ther.–Nucleic Acids* **2012**, *1*, e22.

DOI: 10.1021/acs.joc.6b02417
J. Org. Chem. 2017, 82, 12−24